Rotationally invariant slave-boson formalism and momentum dependence of the quasiparticle weight

Frank Lechermann,[1,2,*] Antoine Georges,[2] Gabriel Kotliar,[2,3] and Olivier Parcollet[4]
[1]*I. Institut für Theoretische Physik, Universität Hamburg, Jungiusstrasse 9, 20355 Hamburg, Germany*
[2]*Centre de Physique Théorique, École Polytechnique, 91128 Palaiseau Cedex, France*
[3]*Serin Physics Laboratories, Rutgers University, Piscataway, New Jersey 08854, USA*
[4]*Service de Physique Théorique, CEA/DSM/SPhT-CNRS/SPM/URA 2306 CEA Saclay, F-91191 Gif-Sur-Yvette, France*
(Received 11 April 2007; revised manuscript received 2 August 2007; published 1 October 2007)

We generalize the rotationally invariant formulation of the slave-boson formalism to multiorbital models, with arbitrary interactions, crystal fields, and multiplet structure. This allows for the study of multiplet effects on the nature of low-energy quasiparticles. Nondiagonal components of the matrix of quasiparticle weights can be calculated within this framework. When combined with cluster extensions of dynamical mean-field theory, this method allows us to address the effects of spatial correlations, such as the generation of the superexchange and the momentum dependence of the quasiparticle weight. We illustrate the method on a two-band Hubbard model, a Hubbard model made of two coupled layers, and a two-dimensional single-band Hubbard model (within a two-site cellular dynamical mean-field approximation).

DOI: 10.1103/PhysRevB.76.155102 PACS number(s): 71.10.Fd, 71.30.+h, 74.25.Jb

I. INTRODUCTION AND MOTIVATIONS

A. General motivations

The method of introducing auxiliary bosons in order to facilitate the description of interacting fermionic systems is an important technique in theoretical many-body physics. In this regard, the so-called slave-boson (SB) approach is a very useful tool in dealing with models of strongly correlated electrons. Slave-boson mean-field theory (SBMFT), i.e., at the saddle-point level, is the simplest possible realization of a Landau Fermi liquid (for a review, see, e.g., Ref. 1). Within SBMFT, a simplified description of the low-energy quasiparticles is obtained, while high-energy (incoherent) excitations are associated with fluctuations around the saddle point. In particular, two essential features are captured by SBMFT: (i) the Fermi surface (FS) of the interacting system (satisfying Luttinger's theorem) is determined by the zero-frequency self-energy, which is in turn determined by the Lagrange multipliers associated with the constraints and (ii) the quasiparticle (QP) weight Z is determined by the saddle-point values of the slave bosons. Hence SBMFT is a well-tailored technique when attempting to understand the low-energy physics emerging from more sophisticated theoretical tools, such as dynamical mean-field theory (DMFT), which deals with the full frequency dependence of the self-energy.

In this paper, we are concerned with the construction of a slave-boson formalism which is able to deal with the two following problems.

(1) In multiorbital models, we handle an arbitrary form of the interaction Hamiltonian, not restricted to density-density terms, and possibly including interorbital hoppings or hybridizations. We aim, in particular, at describing correctly the multiplets (eigenstates of the atomic Hamiltonian), but we also want to be able to work in an arbitrary basis set, not necessarily that of the atomic multiplets (and of course, to obtain identical results, independent of the choice of basis).

(2) We describe situations in which the QP weight is *not* uniform along the Fermi surface, but instead varies as a function of the momentum, i.e., $Z=Z(\mathbf{k})$.

There are clear physical motivations for addressing each of these issues. The first one is encountered whenever one wants to deal with a specific correlated material in a realistic setting (see, e.g., Ref. 2). Usually, more than one band is relevant to the physics (e.g., a t_{2g} triplet or e_g doublet for transition metal oxides, or the full sevenfold set of f orbitals in rare earth, actinides, and their compounds). The second issue is an outstanding one in connection with cuprate superconductors. In those materials, a strong differentiation in momentum space is observed in the "normal" (i.e., nonsuperconducting) state, especially in the underdoped regime (for a review, see, e.g., Ref. 3). For momenta close to the nodal regions, i.e., close to the regions where the superconducting gap vanishes, reasonably long-lived QPs are found. In contrast, in the antinodal directions, the angle-resolved photoemission spectra (ARPES) reveal only a broad line shape with no well-defined QPs. The nature of the incipient normal state in the underdoped regime (i.e., the state achieved by suppressing the intervening superconductivity) has been a subject of debate. One possibility is that QPs would eventually emerge at low-enough temperature in the antinodal region as well, but with a much smaller QP weight $Z_{\mathrm{AN}} \ll Z_{\mathrm{N}}$. Another possibility is that coherent QPs simply do not emerge in the antinodal region. Anyhow, there is evidence from ARPES and other experiments[3] that the QP weight (whenever it can be defined) has significant variation along the FS and is larger at the nodes. Since the QP weight sets the scale for the coherence temperature below which long-lived QPs form, a smaller Z means a smaller coherence temperature. Hence, if the temperature is higher than the coherence scale associated with momenta close to the nodes, and larger than the one associated with the antinodes, QPs will be visible only in the nodal regions. At this temperature, the FS will thus appear as being formed of "Fermi arcs," as indeed observed experimentally.[4] Important differences between the nodal and antinodal regions in the superconducting state have also been unraveled by recent experiments, in particular, from Raman scattering which revealed two different en-

ergy scales with different doping dependences, associated with each of these regions.[5] Momentum-space differentiation of QP properties is therefore a key feature of cuprate superconductors, but it is also an issue which is particularly difficult to handle theoretically.

As we now explain, these two issues are actually closely related one to the other. In a general multiorbital model, the self-energy is a matrix $\Sigma_{\alpha\beta}$ (α and β are orbital indices). Except when a particular symmetry dictates otherwise, this matrix has in general off-diagonal (interorbital) components and these off-diagonal components may have a nonzero linear term in the low-frequency expansion, hence yielding nondiagonal components of the matrix of QP weights defined as

$$\hat{Z} = \left(1 - \frac{\partial}{\partial \omega}\hat{\Sigma}\right)^{-1}_{\omega=0}. \tag{1}$$

On the other hand, a momentum-dependent QP weight $Z(\mathbf{k})$ means that, in real space, $Z_{ij}=Z(\mathbf{R}_i-\mathbf{R}_j)$ depends on the separation between lattice sites (a momentum-independent Z means that $Z_{ij}=Z\delta_{ij}$ is purely local). Hence, in both cases, one has to handle a QP weight which is a matrix in either the orbital or the site indices. The connection becomes very direct in the framework of cluster extensions of DMFT (for reviews, see, e.g., Refs. 6–9). There, a lattice problem is mapped onto a finite-size cluster which is self-consistently coupled to an environment. This finite-size cluster can be viewed as a multiorbital (or molecular) quantum impurity problem, in which each site plays the role of an atomic orbital. Recently, numerical solutions of various forms of cluster extensions to the DMFT equations for the two-dimensional Hubbard model have clearly revealed the phenomenon of momentum-space differentiation.[10–12] Developing low-energy analytical tools to interpret, understand, and generalize the results of these calculations is clearly an important and timely issue. The slave-boson methods developed in the present work are a step in this direction.

Obviously, the existence of off-diagonal components of the $\hat{Z}$ matrix is a basis-set dependent issue. A proper choice of orbital basis can be made, which diagonalizes this matrix. In certain cases, this basis is dictated by symmetry considerations, while in the absence of symmetries, the basis set in which Z is diagonal cannot be guessed *a priori*. For instance, in a two-site cluster or two-orbital model in which the two sites play equivalent roles, even and odd combinations diagonalize not only the $\hat{Z}$ matrix, but, in fact, the self-energy matrix itself for all frequencies (see Sec. III). In such cases, it may be favorable to work in this orbital basis set, and deal only with diagonal QP weights. However, performing the rotation into this orbital basis set will in general transform the interacting Hamiltonian into a more complicated form. For example, starting from a density-density interaction, it may induce interaction terms which are not of the density-density type (i.e., involve exchange, pair hopping, etc.). For these reasons, it is essential to consider slave-boson formalisms which can handle both arbitrary interaction terms, and nondiagonal components of the QP weight matrix: these two issues are indeed connected. The formalism presented in this paper builds on earlier ideas of Wölfle and co-workers[13,14] (see Appendix A), in which the SB formalism is formulated in a *fully rotationally invariant manner* (see also Refs. 15 and 16 in the framework of the Gutzwiller approximation), so that the orbital basis set needs not be specified from the beginning, and the final results are guaranteed to be equivalent irrespectively of the chosen basis set.

B. Some notations

In this paper, we shall consider multiorbital models of correlated electrons with Hamiltonians of the form

$$H = H_{\text{kin}} + \sum_i H_{\text{loc}}[i] \tag{2}$$

with

$$H_{\text{kin}} = \sum_{\mathbf{k}} \sum_{\alpha\beta} \varepsilon_{\alpha\beta}(\mathbf{k}) d^\dagger_{\mathbf{k}\alpha} d_{\mathbf{k}\beta}. \tag{3}$$

In these expressions, α and β label electronic species and run from 1 to M [i.e., M is twice the number of atomic orbitals in the context of a multiorbital model of electrons with spin: $\alpha=(m,\sigma), \sigma=\uparrow,\downarrow$]. The k vector runs over the Brillouin zone of the lattice, whose sites are labeled by i (in the context of cluster DMFT, i will label clusters and runs over the superlattice sites, thus $\mathbf{k}$ runs over the reduced Brillouin zone of the superlattice, see Sec. III C). The first term in Eq. (2) is the kinetic energy: $\varepsilon_{\alpha\beta}(\mathbf{k})$ is the Fourier transform of the (possibly off-diagonal) hoppings and does not contain any local terms [i.e., $\Sigma_{\mathbf{k}}\varepsilon_{\alpha\beta}(\mathbf{k})=0$]. H_{loc} contains both the one-body local terms and the interactions, assumed to be local. A general form for H_{loc} is[55]

$$H_{\text{loc}} = \sum_{\alpha\beta} \varepsilon^0_{\alpha\beta} d^\dagger_\alpha d_\beta + \frac{1}{2} \sum_{\alpha\beta\gamma\delta} U_{\alpha\beta\gamma\delta} d^\dagger_\alpha d^\dagger_\beta d_\delta d_\gamma. \tag{4}$$

Fock states form a convenient basis set of the local Hilbert space on each site. They are specified by sequences $n=(n_1,\ldots,n_M)$, with $n_\alpha=0,1$ (we consider a single site and drop the site index) as follows:

$$|n\rangle = (d^\dagger_1)^{n_1} \cdots (d^\dagger_M)^{n_M} |\text{vac}\rangle. \tag{5}$$

In the following, $\{|A\rangle\}$ will denote an arbitrary basis set of the local Hilbert space, specified by its components on the Fock states as follows

$$|A\rangle = \sum_n \langle n|A\rangle |n\rangle, \tag{6}$$

while $|\Gamma\rangle$ will denote the eigenstates of the local Hamiltonian, i.e., the "atomic" multiplets such that

$$H_{\text{loc}}|\Gamma\rangle = E_\Gamma |\Gamma\rangle. \tag{7}$$

C. Slave bosons for density-density interactions: A reminder

When the orbital densities n_α are good quantum numbers for the local Hamiltonian H_{loc}, i.e., when the eigenstates of the latter are labeled by n_α, a very simple slave-boson for-

malism can be constructed which is a direct multiorbital generalization of the four-boson scheme introduced by Kotliar and co-workers.[17,18] While this is standard material, we feel appropriate to briefly remind the reader of how this scheme works, in order to consider generalizations later on. We thus specialize in this subsection to a local Hamiltonian of the form

$$H_{\mathrm{loc}} = \sum_{\alpha} \varepsilon_{\alpha}^{0} \hat{n}_{\alpha} + \sum_{\alpha\beta} U_{\alpha\beta} \hat{n}_{\alpha} \hat{n}_{\beta}, \tag{8}$$

so that the multiplets are the Fock states $|n\rangle$ themselves, with eigenenergies

$$E_n = \sum_{\alpha} \varepsilon_{\alpha}^{0} n_{\alpha} + \sum_{\alpha\beta} U_{\alpha\beta} n_{\alpha} n_{\beta}. \tag{9}$$

To each Fock state, one associates a boson creation operator $\phi_n^{\dagger}$. Furthermore, auxiliary fermions $f_{\alpha}^{\dagger}$ are introduced which correspond to *quasiparticle degrees of freedom*. The (local) enlarged Hilbert space thus consists of states which are built from tensor products of a QP Fock state, times an arbitrary number of bosons. In contrast, the *physical Hilbert space* is generated by the basis set consisting of the 2^M states which contain exactly one boson, and in which this boson matches the QP Fock state. Thus, the states representing the original physical states (5) in the enlarged Hilbert space, in a one-to-one manner, are the following ("physical") states:

$$|\underline{n}\rangle \equiv \phi_n^{\dagger} |\mathrm{vac}\rangle \otimes |n\rangle_f. \tag{10}$$

The underlining in $|\underline{n}\rangle$ allows one to distinguish between the original Fock state of the physical electrons $|n\rangle$, and its representative state in the enlarged Hilbert space. In this expression, $|n\rangle_f$ stands for the QP Fock state as follows:

$$|n\rangle_f \equiv (f_1^{\dagger})^{n_1} \cdots (f_M^{\dagger})^{n_M} |\mathrm{vac}\rangle. \tag{11}$$

It is easily checked that a simple set of constraints uniquely specifies the physical states among all the states of the enlarged Hilbert space, namely,

$$\sum_{n} \phi_n^{\dagger} \phi_n = 1, \tag{12}$$

$$\sum_{n} n_{\alpha} \phi_n^{\dagger} \phi_n = f_{\alpha}^{\dagger} f_{\alpha}, \quad \forall\ \alpha. \tag{13}$$

The first constraint imposes that only states with a single boson are retained, while the second one ensures that the fermionic (QP) and bosonic contents match. Obviously, the saddle-point values of the slave bosons will have a simple interpretation, $|\phi_n|^2$ being the probability associated with the Fock space configuration n.

The operator

$$\underline{d}_{\alpha}^{\dagger} = \sum_{nm} \langle n | f_{\alpha}^{\dagger} | m \rangle \phi_n^{\dagger} \phi_m f_{\alpha}^{\dagger} \tag{14}$$

is a faithful representation of the physical electron creation operator on the representatives (10), namely,

$$\underline{d}_{\alpha}^{\dagger} |\underline{n}\rangle = \sum_{n'} \langle n' | d_{a}^{\dagger} | n \rangle |\underline{n}'\rangle, \tag{15}$$

in which, in fact, the right-hand side (rhs) is either zero (if $n_{\alpha}=1$) or composed of just a single state (with $n'_{\alpha}=1$ and otherwise $n_{\beta}=n'_{\beta}$ for $\beta \neq \alpha$). This expression of the physical electron operators is not unique; however, obviously, one can, for example, multiply this with any operator acting as the identity on the physical states. This is true as long as the constraint is treated exactly. When treated in the mean-field approximation, however (i.e., at saddle point), these equivalent expressions will not lead to the same results. In fact, Eq. (14) suffers from a serious drawback, namely, it does not yield the exact noninteracting ($U_{\alpha\beta}=0$) limit at saddle point. Instead, the expression

$$\underline{d}_{\alpha}^{\dagger} = \sum_{nm} \langle n | f_{\alpha}^{\dagger} | m \rangle [\hat{\Delta}_{\alpha}]^{-1/2} \phi_n^{\dagger} \phi_m [1 - \hat{\Delta}_{\alpha}]^{-1/2} f_{\alpha}^{\dagger} \tag{16}$$

with

$$\hat{\Delta}_{\alpha}[\phi] \equiv \sum_{n} n_{\alpha} \phi_n^{\dagger} \phi_n \tag{17}$$

turns out to satisfy this requirement, while having exactly the same action as Eq. (14) when acting on physical states. This choice of normalization is actually very natural given the probabilistic interpretation of $|\phi_n|^2$: the expression $[\hat{\Delta}_{\alpha}]^{-1/2} \phi_n^{\dagger}$ ($\phi_m [1 - \hat{\Delta}_{\alpha}]^{-1/2}$) is actually a probability amplitude, normalized over the *restricted set* of physical states such that $n_{\alpha}=1$ ($n_{\alpha}=0$). Hence the combination of boson fields in Eq. (16) is a transition probability between the state m with $m_{\alpha}=0$ and the state n with $n_{\alpha}=1$.

Anyhow, whether the simplest expression (14) or the normalized expression (16) is chosen for the physical operator, the relation between the physical and QP single-particle operators is of the form

$$d_{\alpha} = \hat{r}_{\alpha}[\phi] f_{\alpha}. \tag{18}$$

It is important to note that the orbital index carried by the physical operator is identical to that of the QP operator. An immediate consequence is that the self-energy at the saddle-point level is a *diagonal matrix in orbital space* $\Sigma_{\alpha\beta} = \delta_{\alpha\beta} \Sigma_{\alpha}$, which reads

$$\Sigma_{\alpha}(\omega) = \Sigma_{\alpha}(0) + \omega \left(1 - \frac{1}{Z_{\alpha}} \right) \tag{19}$$

with

$$Z_{\alpha} = |r_{\alpha}|^2, \tag{20}$$

$$\Sigma_{\alpha}(0) = \lambda_{\alpha} / |r_{\alpha}|^2 - \varepsilon_{\alpha}^{0}. \tag{21}$$

In these expressions, r_{α} is evaluated at saddle-point level, and λ_{α} is the saddle-point value of the Lagrange multipliers enforcing the constraint (13).

The expression (20) of the QP weight is an immediate consequence of Eq. (18): at saddle-point level, r_{α} becomes a c number and Eq. (18) implies that the physical electron carries a spectral weight $|r_{\alpha}|^2$. Hence, in order to describe within SBMFT situations in which the QP weight is a non-

diagonal matrix, one must disentangle the orbital indices carried by the physical electron and those carried by the QP degrees of freedom. These operators will then be related by a nondiagonal matrix

$$d_\alpha = \hat{R}_{\alpha\beta}[\phi] f_\beta. \tag{22}$$

This is precisely what the formalism exposed in this paper achieves. The physical significance of such a nondiagonal relation is that creating a physical electron in a given orbital may induce the creation of QPs in any other orbital. Thinking of orbital as real-space indices (within, e.g., cluster DMFT), this means that the creation of a physical electron on a given site induces QPs on other sites in a nonlocal manner, corresponding to a momentum-dependent $Z(\mathbf{k})$.

D. Difficulties with naive generalizations to the multiorbital case

Let us come back to the general multiorbital interaction (4). In order to motivate the fully rotationally invariant formalism exposed in the next section, let us point out some difficulties arising when attempting to generalize the simple SB formalism of the previous section.

The central difference between the general interaction (4) and the density-density form (8) is that the atomic multiplets $|\Gamma\rangle$ are no longer Fock states. Thus, it would seem natural to associate a slave boson ϕ_Γ to each of the atomic multiplets. Indeed, Bünemann *et al.*[19] (see also Ref. 15) have proposed generalized Gutzwiller wave functions in which a variational parameter (also known as a probability $|\phi_\Gamma|^2$) is associated with each atomic multiplet (see also Ref. 20 and the recent work of Dai *et al.*[21] in the SB context). A slave-boson formulation requires a clear identification of the physical states within the enlarged Hilbert space. A natural idea is to define those in one-to-one correspondence with the atomic multiplets, as

$$|\underline{\Gamma}\rangle \overset{?}{=} \phi_\Gamma^\dagger |\mathrm{vac}\rangle \otimes \sum_n \langle n|\Gamma\rangle |n\rangle_f. \tag{23}$$

The local part of the Hamiltonian has a simple representation on these physical states $H_{\mathrm{loc}}=\Sigma_\Gamma E_\Gamma \phi_\Gamma^\dagger \phi_\Gamma$. However, a major difficulty is that there is no simple constraint implementing the restriction to these physical states, and such that it is quadratic in the fermionic (QP) degrees of freedom (which is essential in order to yield a manageable saddle point). In particular, it is easily checked that the apparently natural constraint[21]

$$f_\alpha^\dagger f_\alpha \overset{?}{=} \sum_\Gamma \langle \Gamma|\hat{n}_\alpha|\Gamma\rangle \phi_\Gamma^\dagger \phi_\Gamma \tag{24}$$

is actually not satisfied by the states (23) as an operator identity.[56] Further difficulties also arise when attempting to derive an expression for the physical creation operators. These difficulties stem from the fact that two atomic multiplets having particle numbers differing by one unit cannot in general be related by the action of a single-fermion creation.

One might also think of defining the physical states in correspondence to the Fock states, as:

$$|\underline{n}\rangle \overset{?}{=} |n\rangle_f \otimes \sum_\Gamma \langle \Gamma|n\rangle \phi_\Gamma^\dagger |\mathrm{vac}\rangle, \tag{25}$$

which do satisfy the following quadratic constraint:

$$f_\alpha^\dagger f_\alpha = \sum_{\Gamma\Gamma'} \langle \Gamma|\hat{n}_\alpha|\Gamma'\rangle \phi_\Gamma^\dagger \phi_{\Gamma'}. \tag{26}$$

However, another difficulty then arises. Namely, it is not possible to write the local interaction Hamiltonian purely in terms of bosonic degrees of freedom, which is the whole purpose of SB representations. In particular, the obvious expression $H_{\mathrm{loc}}=\Sigma_\Gamma E_\Gamma \phi_\Gamma^\dagger \phi_\Gamma$ which had the correct action on states (23) no longer works for states (25) since it leaves unchanged the fermionic content of them.

After some thinking, one actually realizes that these naive generalizations are all faced with the same problem, namely, that they do not embody the crucial conceptual distinction between physical and QP degrees of freedom. Both Eqs. (23) and (25) assume *a priori* a definite relation between the physical and QP contents of a state. The key to a successful SB formalism is therefore to *disentangle physical and quasiparticle degrees of freedom*, and letting the variational principle at saddle point decide which relationship actually exists between those.

We shall see, however, in Sec. III A that, provided the local Hamiltonian *has enough symmetries*, the rotationally invariant formalism of the present paper does correspond to assigning at saddle point a probability to each atomic configuration (multiplet) $|\Gamma\rangle$, hence establishing contact with the previous works of Refs. 19 and 21. Yet for less symmetric Hamiltonians, the general formalism of the present paper is requested.

II. ROTATIONALLY INVARIANT SLAVE-BOSON FORMALISM

A. Physical Hilbert space and constraints

In order to construct a SB formalism in which physical and QP states are disentangled, we shall associate a slave boson $\phi_{\Gamma n}$ to *each pair* of atomic multiplet $|\Gamma\rangle$ and QP Fock state $|n\rangle_f$. More generally, we can work in an arbitrary basis set $|A\rangle$ of the local Hilbert space, not necessarily that of the atomic multiplets, and consider slave bosons ϕ_{An}. As we shall see, the formalism introduced in this paper is such that two different choices of basis sets are related by a unitary transformation and therefore lead to identical results. In particular, one could also choose the physical Fock states $|m\rangle_d$ as the basis set A, and work with slave bosons ϕ_{mn} which form the components of a *density matrix* connecting the physical and QP spaces. It is crucial, however, to keep in mind that the first index (A) refers to *physical electron states*, while the second one (n) refers to *quasiparticles*.

A priori, a slave boson ϕ_{An} can be introduced for any pair (A,n). However, in this paper, we shall restrict ourselves to phases which do not display an off-diagonal superconducting long-range order, and hence one can restrict the ϕ_{An}'s to pairs of states which have the same total particle number on a given site (the local Hamiltonian H_{loc} commutes with

$\Sigma_\alpha d_\alpha^\dagger d_\alpha$). The formalism is easily extended to superconducting states[14,15,22] by lifting this assumption and modifying appropriately the expressions derived in this section. In the following, we consider basis states A which are eigenstates of the local particle number (denoted by N_A), and hence a ϕ_{An} is introduced provided $\Sigma_\alpha n_\alpha = N_A$.

The representation of such a basis state in the enlarged Hilbert space is defined as

$$|\underline{A}\rangle \equiv \frac{1}{\sqrt{D_A}} \sum_n \phi_{An}^\dagger |\text{vac}\rangle \otimes |n\rangle_f. \tag{27}$$

In this expression, D_A denotes the dimension of the subspace of the Hilbert space with particle number identical to that of A, i.e., $D_A \equiv D(N_A) = \binom{M}{N_A}$. This ensures a proper normalization of the state. As before, the "underline" in $|\underline{A}\rangle$ allows us to distinguish this state, which lives in the tensor product Hilbert space of QP and boson states, from the physical electron state $|A\rangle$.

Having decided on the physical states, we need to identify a set of constraints which select these physical states out of the enlarged Hilbert space in a necessary and sufficient manner. It turns out that the following (M^2+1) constraints achieve this goal:

$$\sum_{An} \phi_{An}^\dagger \phi_{An} = 1, \tag{28}$$

$$\sum_A \sum_{nn'} \phi_{An'}^\dagger \phi_{An} \langle n | f_\alpha^\dagger f_{\alpha'} | n' \rangle = f_\alpha^\dagger f_{\alpha'}, \quad \forall\, \alpha. \tag{29}$$

The first constraint is obvious and requires that the physical states are single-boson states. It is easy to check that the physical states satisfy the second set of constraints (29), but a little more subtle to actually prove that this set of constraints is sufficient to uniquely select the physical states (27) in the enlarged Hilbert space. The detailed proof is given in Appendix B. Let us emphasize that the order of primed and unprimed indices in Eq. (29) is of central importance.

B. Representation of the physical electron operators

We now turn to the representation of the physical electron creation operator on the representatives (27) of the physical states in the enlarged Hilbert space. We need to find an operator which acts on these representatives exactly as $d_\alpha^\dagger$ acts on the physical basis $|A\rangle$. Namely, given the matrix elements $\langle A | d_\alpha^\dagger | B \rangle$ such that

$$d_\alpha^\dagger |B\rangle = \sum_A \langle A | d_\alpha^\dagger | B \rangle |A\rangle, \tag{30}$$

we want to find an operator $\underline{d}_\alpha^\dagger$ (in terms of the boson and QP operators) such that

$$\underline{d}_\alpha^\dagger |\underline{B}\rangle = \sum_A \langle A | d_\alpha^\dagger | B \rangle |\underline{A}\rangle. \tag{31}$$

1. Proximate expression

As in the case of the density-density interactions discussed above (Sec. I C), the answer is not unique. We first construct the generalization of expression (14) to the present formalism (i.e., ignore at first the question of the proper operators to be inserted in order to recover the correct noninteracting limit). The following expression is shown in Appendix C to satisfy Eq. (31):

$$\underline{d}_\alpha^\dagger = \sum_{\beta,AB,nm} \frac{\langle A | d_\alpha^\dagger | B \rangle \langle n | f_\beta^\dagger | m \rangle}{\sqrt{N_A (M - N_B)}} \phi_{An}^\dagger \phi_{Bm} f_\beta^\dagger. \tag{32}$$

We note that $N_A = N_B + 1$ in this expression can take the values $1, \ldots, M$.

Hence, we see that within this formalism, the physical and QP operators are indeed related by a nondiagonal transformation (22) as follows:

$$\underline{d}_\alpha = \hat{R}[\phi]_{\alpha\beta} f_\beta \tag{33}$$

with the $\hat{R}$ matrix corresponding to Eq. (32) given by ($\hat{R}^*_{\alpha\beta}$ denotes the complex conjugate of $\hat{R}_{\alpha\beta}$)

$$\hat{R}[\phi]^*_{\alpha\beta} = \sum_{AB,nm} \frac{\langle A | d_\alpha^\dagger | B \rangle \langle n | f_\beta^\dagger | m \rangle}{\sqrt{N_A (M - N_B)}} \phi_{An}^\dagger \phi_{Bm}. \tag{34}$$

The action of Eq. (32) on physical states, and the proof that it satisfies Eq. (31) are detailed in Appendix C.

2. Improved expression

The simple expression (32), although having the correct action on the physical states, suffers from the same drawback than Eq. (14) in the case of density-density interactions. Namely, at saddle-point level (i.e., with the constraint satisfied on average instead of exactly), the noninteracting limit is not appropriately recovered. Thus, one needs to generalize the improved expression (16) to the present rotationally invariant formalism. However, care must be taken to do so in a way which respects gauge invariance (i.e., the possibility of making an arbitrary unitary rotation on the QP orbital indices, see Sec. II C).

We consider the following operators, bilinear in the bosonic fields:

$$\hat{\Delta}^{(p)}_{\alpha\beta} \equiv \sum_{Anm} \phi_{An}^\dagger \phi_{Am} \langle m | f_\alpha^\dagger f_\beta | n \rangle, \tag{35}$$

$$\hat{\Delta}^{(h)}_{\alpha\beta} \equiv \sum_{Anm} \phi_{An}^\dagger \phi_{Am} \langle m | f_\beta f_\alpha^\dagger | n \rangle, \tag{36}$$

which can be interpreted as particle- and holelike QP density matrices (note that when the constraint is satisfied exactly, $\hat{\Delta}^{(h)}_{\alpha\beta} = \delta_{\alpha\beta} - \hat{\Delta}^{(p)}_{\alpha\beta}$). We then choose to modify the R matrix in the following manner (see Appendix C):

$$\hat{R}[\phi]^*_{\alpha\beta} = \sum_{AB,nm,\gamma} \langle A | d_\alpha^\dagger | B \rangle \langle n | f_\gamma^\dagger | m \rangle \phi_{An}^\dagger \phi_{Bm} M_{\gamma\beta} \tag{37}$$

with

$$M_{\gamma\beta} \equiv \langle \gamma | \left[\tfrac{1}{2} (\hat{\Delta}^{(p)} \hat{\Delta}^{(h)} + \hat{\Delta}^{(h)} \hat{\Delta}^{(p)}) \right]^{-1/2} | \beta \rangle. \tag{38}$$

We chose to let the QP density matrices enter the M matrix in a symmetrized way in order to respect equivalent treat-

ment of particles and holes. Expression (37) can be shown to be gauge invariant, and turns out to yield the correct noninteracting limit at saddle point. However, although it yields a saddle point satisfying all the appropriate physical requirements, it is not fully justified as an operator identity.

C. Gauge invariance

As usual in formalisms using slave particles, a *gauge symmetry* is present which allows one to freely rotate the QP orbital indices, independently on each lattice site. Physical observables are of course gauge invariant. Let us consider an arbitrary SU(M) rotation of the QP operators as follows:

$$f_\alpha^\dagger = \sum_\beta U_{\alpha\beta} \tilde{f}_\beta^\dagger. \tag{39}$$

This rotation induces a corresponding unitary transformation $\mathcal{U}(U)$ of the QP Fock states $|n\rangle_f$. This unitary transformation is characterized by the fact that the expectation value of f_α in its Fock basis is an invariant tensor: it is the same in every basis. Therefore (summation over repeated indices is implicit everywhere in the following)

$$\langle n|f_\beta^\dagger|m\rangle = U_{\beta\beta'}\mathcal{U}(U)^*_{nn'}\langle n'|f_{\beta'}^\dagger|m'\rangle\mathcal{U}(U)_{mm'}, \tag{40}$$

$$\langle n|f_\alpha^\dagger f_\beta|m\rangle = U_{\alpha\alpha'}U^*_{\beta\beta'}\mathcal{U}^*(U)_{nn'}\langle n'|f_{\alpha'}^\dagger f_{\beta'}|m'\rangle\mathcal{U}(U)_{mm'} \tag{41}$$

(the second expression can be deduced from the first using closure relations). We can now check that if the slave bosons transforms like

$$\phi_{An} = \mathcal{U}(U)_{nn'}\tilde{\phi}_{An'}, \tag{42}$$

then the constraints and the expressions of the physical electron operator [either Eq. (32) or Eq. (37)] are gauge invariant. Namely, the R matrix obeys the following transformation law:

$$\hat{R}[\phi]_{\alpha\beta} = \hat{R}[\tilde{\phi}]_{\alpha\beta'}U_{\beta\beta'} \tag{43}$$

and therefore the physical electron operator is invariant,

$$d_\alpha = \hat{R}[\tilde{\phi}]_{\alpha\beta}\tilde{f}_\beta = \hat{R}[\phi]_{\alpha\beta}f_\beta. \tag{44}$$

D. Change of physical and quasiparticle basis sets

It is clear that the basis $|A\rangle$ of the local Hilbert space (i.e., the physical basis states) can be chosen arbitrarily in this formalism. Indeed, making a basis change from $|A\rangle$ to $|\tilde{A}\rangle$, all the expressions above keep an identical form provided the bosons corresponding to the new basis are defined as

$$\phi_{\tilde{A}n}^\dagger = \sum_A \langle A|\tilde{A}\rangle\phi_{An}^\dagger. \tag{45}$$

As mentioned above, it is often convenient to use the eigenstates $|\Gamma\rangle$ of $H_{\rm loc}$ as a basis set.

Changing the basis states associated with *quasiparticles* is a somewhat trickier issue. Up to now, we have worked with Fock states $|n\rangle_f$. A different basis set $|Q\rangle_f$ can be used, provided, however, the unitary matrix $\langle Q|n\rangle$ is *real*, i.e., $\langle Q|n\rangle = \langle n|Q\rangle$. Indeed, the matrix element $\langle Q|n\rangle$ appears in the transformation of the physical states and of the constraint, while $\langle n|Q\rangle$ appears in the transformation of the physical electron operator. When this matrix elements are real, new bosons can be defined in the transformed QP basis according to

$$\phi_{AQ}^\dagger = \sum_n \langle Q|n\rangle\phi_{An}^\dagger \quad (\langle Q|n\rangle = \langle n|Q\rangle). \tag{46}$$

In particular, when the local Hamiltonian is a real symmetric matrix, the same linear combinations of Fock states which define the atomic multiplets $|\Gamma\rangle$ can be used for QPs, and bosons $\phi_{\Gamma\Gamma'}$ can be considered. This is sometimes a useful way of interpreting the formalism and the results at saddle point (see Sec. III A).

E. Expression of the Hamiltonian, free energy, and Green's function

In this section, we derive the expression of the Hamiltonian in terms of the slave boson and QP fermionic variables. We then construct the free-energy functional to be minimized within a mean-field treatment, and express the Green's function and self-energy at saddle point.

We recall that the full Hamiltonian (2) reads, in terms of the physical electron variables, $H = H_{\rm kin} + \Sigma_i H_{\rm loc}[i]$ with $H_{\rm kin} = \Sigma_{\mathbf{k}}\Sigma_{\alpha\beta}\varepsilon_{\alpha\beta}(\mathbf{k})d_{\mathbf{k}\alpha}^\dagger d_{\mathbf{k}\beta}$ the intersite kinetic energy and $H_{\rm loc}$ the local part of the Hamiltonian on a given site i, with general form (4).

It is easily checked that the following bosonic operator is a faithful representation of $H_{\rm loc}$ on the representatives of the physical states in the enlarged Hilbert space:

$$\underline{H}_{\rm loc} = \sum_{AB}\langle A|H_{\rm loc}|B\rangle\sum_n \phi_{An}^\dagger\phi_{Bn}. \tag{47}$$

If the basis $|\Gamma\rangle$ of atomic multiplets is used, this simplifies down to

$$\underline{H}_{\rm loc} = \sum_\Gamma E_\Gamma\sum_n \phi_{\Gamma n}^\dagger\phi_{\Gamma n}. \tag{48}$$

Using the bosonic R operators relating the physical electron to the QP operators yields the following expression of the kinetic energy:

$$\underline{H}_{\rm kin} = \sum_{\mathbf{k}}\sum_{\alpha\alpha'\beta\beta'}[\hat{R}^\dagger]_{\alpha\alpha'}\varepsilon_{\alpha'\beta'}(\mathbf{k})\hat{R}_{\beta'\beta}f_{\mathbf{k}\alpha}^\dagger f_{\mathbf{k}\beta}. \tag{49}$$

A mean-field theory is obtained by condensing the slave bosons into c numbers $\langle\phi_{An}\rangle \equiv \varphi_{An}$. The constraints are implemented by introducing Lagrange multipliers: λ_0 associated with Eq. (28) and $\lambda_{\alpha\alpha'} \equiv [\Lambda]_{\alpha\alpha'}$ associated with Eq. (29). The saddle point is obtained by extremalizing, over the φ_{An}'s and the Lagrange multipliers, the following free-energy functional:

$$\Omega[\{\varphi_{An}\};\Lambda,\lambda_0] \tag{50}$$

$$= -\frac{1}{\beta}\sum_{\mathbf{k}} \mathrm{tr}\ \ln[1+\mathrm{e}^{-\beta(\mathbf{R}^\dagger(\varphi)\boldsymbol{\varepsilon}(\mathbf{k})\mathbf{R}(\varphi)+\Lambda)}] - \lambda_0 + \sum_{ABnn'} \varphi^*_{An'}\{\delta_{nn'}\delta_{AB}\lambda_0 + \delta_{nn'}\langle A|H_{\mathrm{loc}}|B\rangle - \delta_{AB}\sum_{\alpha\beta}\Lambda_{\alpha\beta}\langle n|f^\dagger_\alpha f_\beta|n'\rangle\}\varphi_{Bn}. \tag{51}$$

The saddle-point equations, as well as technical aspects of their numerical solution, are detailed in Appendix D.

Finally, we derive the expressions of the Green's functions $\hat{G}$, the self-energy $\hat{\Sigma}$, and the QP weight $\hat{Z}$ at saddle point. For the QPs, the one-particle Green's function $G_{f,\alpha\beta}(\mathbf{k},\tau-\tau') \equiv -\langle f^\dagger_{\mathbf{k}\alpha}(\tau) f_{\mathbf{k}\beta}(\tau')\rangle$ reads (in matrix form)

$$\mathbf{G}_f^{-1}(\mathbf{k},\omega) = \omega - \mathbf{R}^\dagger(\varphi)\boldsymbol{\varepsilon}(\mathbf{k})\mathbf{R}(\varphi) - \boldsymbol{\Lambda}, \tag{52}$$

and hence the physical electron Green's function reads (we drop the φ dependence for convenience)

$$\mathbf{G}_d^{-1}(\mathbf{k},\omega) = [\mathbf{R}^\dagger]^{-1}\mathbf{G}_f^{-1}\mathbf{R}^{-1} = \omega(\mathbf{R}\mathbf{R}^\dagger)^{-1} - [\mathbf{R}^\dagger]^{-1}\boldsymbol{\Lambda}\mathbf{R}^{-1} - \boldsymbol{\varepsilon}(\mathbf{k}), \tag{53}$$

while the noninteracting Green's function is (including the one-body term present in H_{loc})

$$\mathbf{G}_{d0}^{-1}(\mathbf{k},\omega) = \omega\mathbb{1} - \boldsymbol{\varepsilon}^0 - \boldsymbol{\varepsilon}(\mathbf{k}). \tag{54}$$

The physical self-energy is thus

$$\Sigma_d(\omega) \equiv \mathbf{G}_{d0}^{-1} - \mathbf{G}_d^{-1} = \omega(1-[\mathbf{R}\mathbf{R}^\dagger]^{-1}) + [\mathbf{R}^\dagger]^{-1}\boldsymbol{\Lambda}\mathbf{R}^{-1} - \boldsymbol{\varepsilon}^0. \tag{55}$$

So that the matrix of QP weights is obtained in terms of the $\hat{R}$ matrix at saddle point as

$$\mathbf{Z} = \mathbf{R}\mathbf{R}^\dagger. \tag{56}$$

This generalizes Eq. (20) to nondiagonal cases. It is easily checked that these expressions of the physical quantities $\mathbf{G}_d$, Σ_d, and $\mathbf{Z}$ are indeed gauge invariant.

III. ILLUSTRATIVE RESULTS

In the following, we apply the above formalism to three different model problems in strongly correlated physics. First, we consider two popular models, namely, the two-band Hubbard model on a three-dimensional (3D) cubic lattice, and a "bilayer" model, coupling two Hubbard 3D cubic lattices. Finally, a two-site cluster (cluster DMFT) approximation to the single-band Hubbard model on a two-dimensional (2D) square lattice is investigated. Hence these models have in common that they all involve two coupled orbitals [associated, in the cluster-DMFT (CDMFT) framework, to the dimer made of two lattice sites]. The present formalism is of course not restricted to two-orbital problems; however, such models provide the simplest examples where the power of the method may be demonstrated.

A. Two-band Hubbard model

The Hubbard model involving two correlated bands, without further onsite hybridization or crystal-field splitting, serves as one of the standard problems in condensed matter theory. In contrast to the traditional single-band model, the formal interaction term in Eq. (4) now generates in the most general fully SU(2) symmetric case four energy parameters, i.e., the intraorbital Hubbard U and the interorbital Hubbard U' as well as the two exchange couplings J and J_C. Thus the present atomic Hamiltonian reads

$$H_{\mathrm{loc}} = U\sum_\alpha n_{\alpha\uparrow}n_{\alpha\downarrow} + U'\sum_{\sigma\sigma'} n_{1\sigma}n_{2\sigma'} - J\sum_\sigma n_{1\sigma}n_{2\sigma} + J\sum_\sigma d^\dagger_{1\sigma}d^\dagger_{2\bar{\sigma}}d_{1\bar{\sigma}}d_{2\sigma} + J_C(d^\dagger_{1\uparrow}d^\dagger_{1\downarrow}d_{2\downarrow}d_{2\uparrow} + d^\dagger_{2\uparrow}d^\dagger_{2\downarrow}d_{1\downarrow}d_{1\uparrow}). \tag{57}$$

The kinetic energy shall contain only intraband terms for a basic tight-binding (TB) model for s bands on a 3D simple cubic lattice with lattice constant a. Thus the corresponding Hamiltonian is written as

$$H_{\mathrm{kin}} = -\frac{1}{3}\sum_\sigma \sum_{\alpha=1,2} t_\alpha \sum_{i,j} d^\dagger_{i\alpha\sigma}d_{j\alpha\sigma}, \tag{58}$$

with the eigenvalues

$$\varepsilon_\alpha(\mathbf{k}) = -\frac{2}{3}t_\alpha \sum_{\mu=xyz}\cos(k_\mu a), \tag{59}$$

where t_α denotes the hopping parameter for orbital $\alpha=1,2$. For convenience, we set $a=1$. The factor $1/3$ in Eq. (58) is to normalize the total bandwidth to $W_\alpha=4t_\alpha$. Because of the cubic symmetry, $U'=U-2J$ may be used, and furthermore we set $J=J_C$. This model is similar to the one considered by Bünemann *et al.*[19] using a generalized Gutzwiller approximation (see also Ref. 15). Our simpler TB description exhibits in principle perfect nesting; however, this issue is not relevant at the present level. The 3D two-band Hubbard model is studied to make contact with the named previous work and in order to establish the connection between the Gutzwiller and slave-boson points of view.

When working in the SU(2) rotationally invariant case, the $2^4=16$ atomic eigenstates $|\Gamma\rangle$ of the local Hamiltonian (57) serve as the appropriate atomic basis (see Table I); however, also the simpler Fock basis (or any other) may be used. Of course, in the Fock basis, a more complicated energy *matrix* must be used in the saddle-point equations (see Appendix D). It should be clear from Table I that there are 20 nonzero slave-boson amplitudes $\phi_{\Gamma n}$ for the current problem. The $S^z=0$ triplet as well as the three singlets are described with two $\phi_{\Gamma n}$, respectively. In principle, even more $\phi_{\Gamma n}$ may be introduced in the beginning of the iteration cycle to minimize Ω, but at convergence those will come out to be strictly zero. Of course, in high-symmetry situations there is still some redundancy within the set of the 20 SBs. For instance, for equal bandwidth at half-filling (see Fig. 1), all the one- and three-particle SBs are identical, as well as the zero- and four-particle SBs. Moreover the $S^z=\pm1$ triplet SBs are equal

TABLE I. Eigenstates $|\Gamma\rangle$ of the SU(2) rotationally invariant two-band Hubbard model. Spin values and energies are given for the eigenstates. The last column shows the slave bosons for the description of the eigenstates in the SBMFT formalism.

No.	Eigenstate $\|\Gamma\rangle$	S_Γ	S^z_Γ	E_Γ	$\phi_{\Gamma n}$
1	$\|00,00\rangle$	0	0	0	$\phi_{1,\|00,00\rangle}$
2	$\|\uparrow 0,00\rangle$	$\frac{1}{2}$	$\frac{1}{2}$	0	$\phi_{2,\|\uparrow 0,00\rangle}$
3	$\|0\downarrow,00\rangle$	$\frac{1}{2}$	$-\frac{1}{2}$	0	$\phi_{3,\|0\downarrow,00\rangle}$
4	$\|00,\uparrow 0\rangle$	$\frac{1}{2}$	$\frac{1}{2}$	0	$\phi_{4,\|00,\uparrow 0\rangle}$
5	$\|00,0\downarrow\rangle$	$\frac{1}{2}$	$-\frac{1}{2}$	0	$\phi_{5,\|00,0\downarrow\rangle}$
6	$\|\uparrow 0,\uparrow 0\rangle$	1	1	$U'-J$	$\phi_{6,\|\uparrow 0,\uparrow 0\rangle}$
7	$\frac{1}{\sqrt{2}}(\|\uparrow 0,0\downarrow\rangle+\|0\downarrow,\uparrow 0\rangle)$	1	0	$U'-J$	$(\phi_{7,\|\uparrow 0,0\downarrow\rangle},\phi_{7,\|0\downarrow,\uparrow 0\rangle})$
8	$\|0\downarrow,0\downarrow\rangle$	1	−1	$U'-J$	$\phi_{8,\|0\downarrow,0\downarrow\rangle}$
9	$\frac{1}{\sqrt{2}}(\|\uparrow 0,0\downarrow\rangle-\|0\downarrow,\uparrow 0\rangle)$	0	0	$U'+J$	$(\phi_{9,\|\uparrow 0,0\downarrow\rangle},\phi_{9,\|0\downarrow,\uparrow 0\rangle})$
10	$\frac{1}{\sqrt{2}}(\|\uparrow\downarrow,00\rangle-\|00,\uparrow\downarrow\rangle)$	0	0	$U-J_C$	$(\phi_{10,\|\uparrow\downarrow,00\rangle},\phi_{10,\|00,\uparrow\downarrow\rangle})$
11	$\frac{1}{\sqrt{2}}(\|\uparrow\downarrow,00\rangle+\|00,\uparrow\downarrow\rangle)$	0	0	$U+J_C$	$(\phi_{11,\|\uparrow\downarrow,00\rangle},\phi_{11,\|00,\uparrow\downarrow\rangle})$
12	$\|\uparrow\downarrow,\uparrow 0\rangle$	$\frac{1}{2}$	$\frac{1}{2}$	$U+2U'-J$	$\phi_{12,\|\uparrow\downarrow,\uparrow 0\rangle}$
13	$\|\uparrow\downarrow,0\downarrow\rangle$	$\frac{1}{2}$	$-\frac{1}{2}$	$U+2U'-J$	$\phi_{13,\|\uparrow\downarrow,0\downarrow\rangle}$
14	$\|\uparrow 0,\uparrow\downarrow\rangle$	$\frac{1}{2}$	$\frac{1}{2}$	$U+2U'-J$	$\phi_{14,\|\uparrow 0,\uparrow\downarrow\rangle}$
15	$\|0\downarrow,\uparrow\downarrow\rangle$	$\frac{1}{2}$	$-\frac{1}{2}$	$U+2U'-J$	$\phi_{15,\|0\downarrow,\uparrow\downarrow\rangle}$
16	$\|\uparrow\downarrow,\uparrow\downarrow\rangle$	0	0	$2U+4U'-2J$	$\phi_{16,\|\uparrow\downarrow,\uparrow\downarrow\rangle}$

because of the degeneracy. The two SBs describing the $S^z=0$ triplet are also identical, with a magnitude $\phi_{(t,0)n}=\phi_{(t,\pm 1)n}/\sqrt{2}$. Also the bosons describing one specific singlet have the same absolute value; however, they carry the multiplet phase information, i.e., have plus or minus sign. In conclusion, in the orbitally degenerate case, the SB amplitudes at saddle point are of the form

$$\varphi_{\Gamma n}=\langle n|\Gamma\rangle y_\Gamma, \tag{60}$$

in which the matrix element $\langle\Gamma|n\rangle$ is entirely determined by $H_{\rm loc}$ and y_Γ is a (coupling-dependent) amplitude, depending only on the eigenstate Γ. This is more clearly interpreted when atomic states are also used as basis states for QPs (Sec. II D). Indeed, Eq. (60) means that

$$\varphi_{\Gamma\Gamma'}=\delta_{\Gamma\Gamma'}y_\Gamma. \tag{61}$$

Hence, in this highly symmetric case, the saddle point is indeed of the diagonal form considered in Refs. 19 and 21. Once the symmetry is lowered, more SBs become inequivalent and this relation does not hold anymore: there are off-diagonal components even when the basis of atomic states is used for both physical and QP states. In this context, the present formalism becomes essential. Different bandwidths for each orbital, together with a finite doping away from half-filling, lead, for instance, to two different absolute values for the two SBs associated with the singlets formed by the two doubly occupied Fock states (as seen at the end of this paragraph in Fig. 6).

Since no interorbital hybridization is applied in this section, the $\hat{Z}$ matrix is diagonal. We consider first the simple case of equal bandwidths $t_1=t_2=0.5$ (note that in all our applications, t sets the unit of energy), thus $Z_{11}=Z_{22}=Z$. Figure 2 shows the variation of Z for different ratios J/U in the half-filled case ($n=2$). The critical coupling U_c for the Mott transition with $J=0$ obtained from this slave-boson calculation is in accordance with the result of the analytical formula given by Frésard and Kotliar.[18] It is seen that an increased J lowers the critical U and moreover changes the transition from second to first order. Note that in this regard, Fig. 2 depicts Z up to the spinodal boundary, i.e., the true transition (following from an energy comparison) is expected to be at

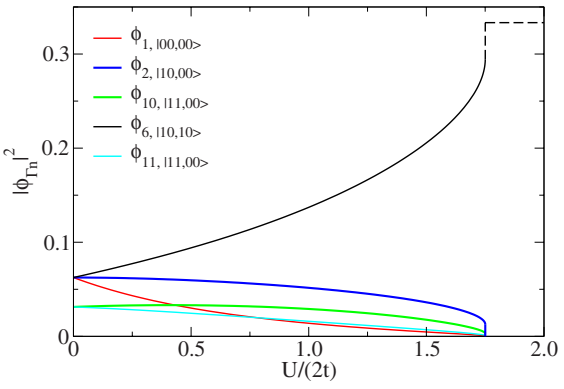

FIG. 1. (Color online) Inequivalent slave-boson probabilities $|\phi_{\Gamma n}|^2$ for the two-band Hubbard model at half-filling for equal bandwidth and $J/U=0.2$. Note that $\phi_{10,|\uparrow\downarrow,00\rangle}$ and $\phi_{11,|\uparrow\downarrow,00\rangle}$ describe part of the singlet states, hence their overall amplitude is scaled by $1/\sqrt{2}$.

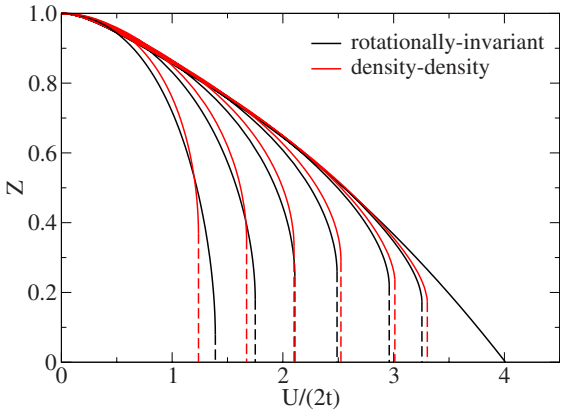

FIG. 2. (Color online) Influence of J on the Mott transition in the two-band Hubbard model at half-filling ($n=2$) for equal bandwidth. From right to left: $J/U=0,0.01,0.02,0.05,0.10,0.20,0.45$.

slightly lower U_c. One can also observe the nonmonotonic character for the evolution of the critical Z at this boundary when increasing J/U. We plot in Fig. 2 additionally the results when restricting the atomic Hamiltonian to density-density terms only, in order to check for the importance of the neglected spin-flip and pair-hopping terms. For larger J/U the critical Z from the latter description is larger compared to the rotationally invariant one and moreover it is monotonically growing. The latter feature strengthens the first-order character in the density-density formulation for growing J/U, whereas for rotationally invariant interactions this character is strongly weakened in that regime. Although for $J/U=0.45$ the jump of Z is quite small, the transition is, however, still first order in the present calculation. Furthermore, there appears to be a crossover between the two approaches concerning the reachable metallic spinodal boundary when increasing J/U.

At quarter filling ($n=1$) a continuous transition is obtained for all the previous interactions (see Fig. 3). Compared to the half-filled case, the density-density approximation appears to be less severe for small J/U, but leads to some differences compared to the rotationally invariant form for large J/U. Note that for $J/U=0.45$, $U'-J$ in the local Hamiltonian (57) becomes negative. Thus a corresponding change of the ground state may lead to the resulting nonmonotonic behavior for U_c then observed in Fig. 3. The critical U for $J=0$ is smaller than at half-filling and with increasing J/U the transition is shifted to *larger* U_c (with the above named exception for J/U large). Hence J has a rather different influence on the degree of correlation for the two fillings. While for $n=2$ Hund's rule coupling substantially enhances the correlations, seen by the decrease in Z, for $n=1$ the opposite effect may be observed. This is also demonstrated in Fig. 4 which displays the influence of J for fixed values of U comparing half-filling with quarter filling. The strong decrease in Z upon increasing J was recently shown to be important for the physical properties of actinides, in particular, regarding the distinct properties of δ-plutonium and curium.[23] For each U shown in Fig. 4, the density-density limiting value $U/3$ was used as an upper bound for J. However, for $U=2$ and $U=3$ the system shows already a first-order transition at half-filling below the latter limit.

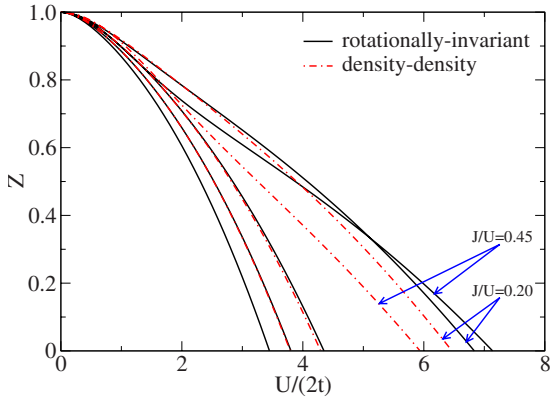

FIG. 3. (Color online) Influence of J on the Mott transition in the two-band Hubbard model at quarter filling ($n=1$) for equal bandwidth. The first three combined curves for the two types of interactions (from left to right) belong to $J/U=0,0.05,0.10$. The arrows indicate the labeling for the two larger J/U ratios.

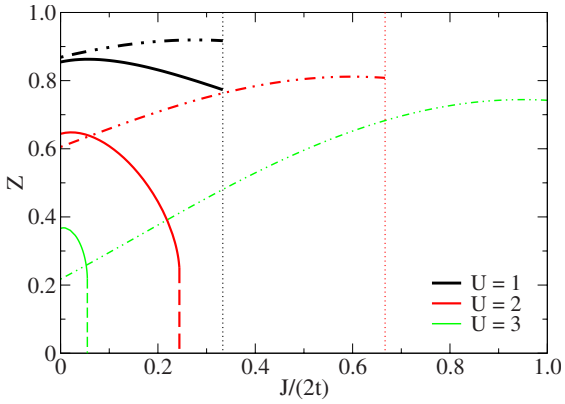

FIG. 4. (Color online) Influence of J for fixed U at $n=2$ (solid lines) and $n=1$ (dotted-dashed lines) for equal bandwidth and full SU(2) symmetry. The vertical dotted lines mark the limit we set for J.

The QP residue Z is shown as a function of filling n in Fig. 5 for $U=1.75$ and three ratios J/U. For $J=0$ it is observed that $Z(n)$ exhibits two minima, both located at integer filling. The minimum at $n=1$ is deeper, corresponding to a lower value for U_c in the quarter-filled case. Because of the filling-dependent effect of J seen in Fig. 4, the nonmonotonic character of $Z(n)$ is lifted for growing J/U.

The two-band Hubbard model was already extensively studied in the more elaborate DMFT framework in infinite dimensions. Such investigations reveal the same qualitative change of the critical U for different integer fillings,[24,25] of course with some minor quantitative differences. Also the reduction[24,26–29] of U_c and the onset of a first-order Mott transition[24,26,27,29] for finite J/U at half-filling is in accordance. Concerning the latter effect, the trend of weakening the first-order tendency for large J/U is also reproduced and there is some discussion[26,27] about the possibility of even changing back to a continuous Mott transition in that regime.

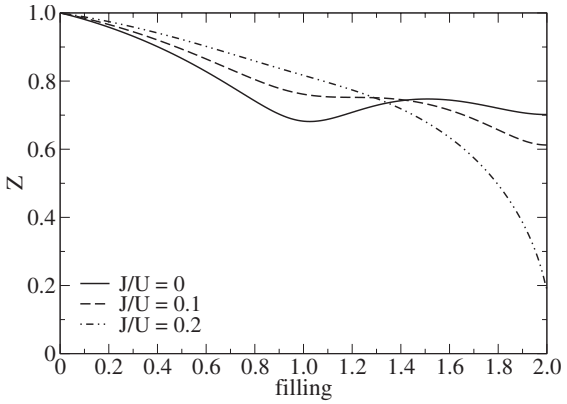

FIG. 5. Filling dependence of Z for selected values of J/U within the equal-bandwidth two-band model with full SU(2) symmetry ($U=1.75$).

The increasing U_c with growing J at quarter filling was also found by Song and Zou.[29]

Finally, in Fig. 6 a comparison between the equal-bandwidth and the different-bandwidth cases at noninteger filling $n=1.5$ is displayed ($J/U=0.2$). For $W_1=W_2$ the model does not show a metal-insulator transition because of the doping. Also the filling of both bands is identical and constant with increasing U ($n_{s1}=n_{s2}=0.375$), and as stated earlier the SBs are still of the form given by Eq. (60). However, when breaking the symmetry between the two bands by considering different bandwidths, the model behaves qualitatively rather differently. The individual band fillings are not identical anymore, favoring the larger-bandwidth band for $U=0$. With increasing U the system manages to drive at least one band insulating by transferring charge from the broader into the narrower band, until the latter is filled with one electron.[30,31] Hence Z_2 of the narrower band becomes zero at

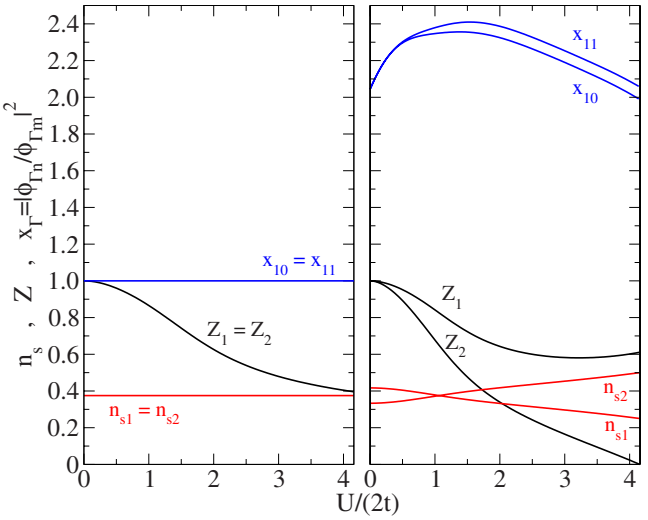

FIG. 6. (Color online) Comparison of the two-band model for $W_1=W_2$ (left) and $W_1=2W_2$ (right) at noninteger filling $n=1.5$ and $J/U=0.2$. The ratio x is plotted for the singlet states coupling the doubly occupied Fock states (see Table I), demonstrating that $\varphi_{\Gamma\Gamma'}$ is no longer diagonal in this case.

an orbital-selective Mott transition (OSMT).[30–35] This asymmetric model has also a more sophisticated SB description, since, for instance, the SBs of the singlets built out of the respective doubly occupied Fock states have now different amplitudes.

B. Hubbard bilayer

Next, we consider a model consisting of two single-band Hubbard models (two "layers"), coupled by an interlayer hopping V. This rather popular model has already been subject of various studies.[36–39] For simplicity and in order to make connection to the previous section, each layer is described here by a 3D cubic lattice, with an onsite repulsion U and an intralayer bandwidth W_α ($\alpha=1,2$), possibly different for the two layers. Hence the local Hamiltonian for this problem reads

$$H_{\mathrm{loc}} = U \sum_{\alpha=1,2} n_{\alpha\uparrow} n_{\alpha\downarrow} + V \sum_{\sigma} (d_{1\sigma}^{\dagger} d_{2\sigma} + d_{2\sigma}^{\dagger} d_{1\sigma}) + \frac{J}{2} \sum_{\sigma\sigma'} d_{1\sigma}^{\dagger} d_{1\sigma'} d_{2\sigma'}^{\dagger} d_{2\sigma}, \tag{62}$$

where the last term describes a possible spin-spin interaction between the layers. However, for simplicity, we only present in this paper results with $J=0$. Our choice of kinetic energy is equivalent to the one in the last section, i.e., given by Eqs. (58) and (59).

In the presence of V, an off-diagonal self-energy $\Sigma_{12}(\omega)$ is generated. Furthermore, away from half-filling ($n_1+n_2=2$), this self-energy is expected to have a term linear in ω at low frequency, and hence $Z_{12}\neq 0$. We note that, when the bandwidths are equal ($W_1=W_2$), the bilayer model can be transformed into a two-orbital model by a $\mathbf{k}$-independent rotation to the bonding-antibonding (or $+,-$) basis. In the latter basis, there is no hybridization but instead a crystal-field splitting ($=2V$) between the two orbitals. The couplings of the two-orbital Hamiltonian are given by (in the notation of the previous section, and for $J=0$) $U_{\mathrm{eff}}=U'_{\mathrm{eff}}=J_{\mathrm{eff}}=U/2$. When the bandwidths are different, the interlayer hopping cannot be eliminated without generating nonlocal interdimer interactions.

Due to the reduced symmetry of the present model in comparison to the two-band Hubbard model from the previous section, the number of nonzero SBs ϕ_{An} equals now 36 (we use here the Fock basis for $|A\rangle$). We first consider the simplest case of a half-filled system ($n_1=n_2=1$) with equal bandwidths $W_1=W_2$ (and $J=0$). Results for the intralayer QP weight and the orbital occupancies of the bonding and antibonding bands are given in Fig. 7. It is seen that the Mott transition is continuous for $V=0$ but becomes discontinuous in the presence of an interlayer hopping $V\neq 0$. For $V=0.25$ the spinodal boundary of the metallic regime is reached for $U\sim 2.055$. These results are consistent with findings in previous works[36–40] within the DMFT framework.

Still focusing on the half-filled case, we display in Fig. 8 the QP weight as a function of U for different bandwidth ratios W_2/W_1. When $V=0$, one has two independent Mott transitions in each layer, i.e., an OSMT scenario, at which Z

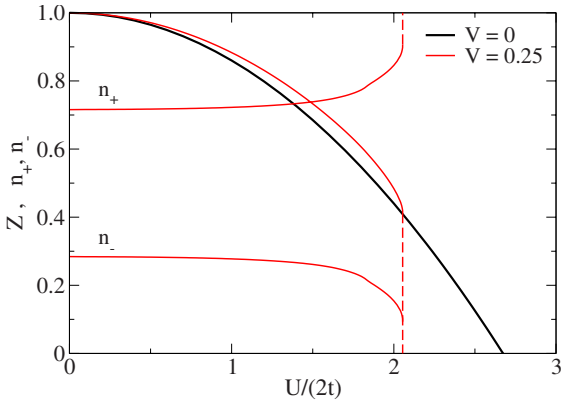

FIG. 7. (Color online) Half-filled bilayer with equal bandwidth for $V=0$ and $V=0.25$. For $V=0$ the filling per spin within the two bands is identical ($n_{s1}=n_{s2}=0.5$), whereas for finite V the symmetry-adapted bonding and/or antibonding states have different filling, denoted n_+, n_-.

vanishes continuously. In the presence of a nonzero V, this is replaced by a *single discontinuous transition* for both orbitals. This is consistent with previous findings on the OSMT problem.[32]

We now consider the effect of finite doping away from half-filling. Figure 9 displays the diagonal ($Z_{11}=Z_{22}$) elements as well as the now appearing Z_{12} element of the QP weight matrix as a function of doping for $U<U_c$. Additionally shown are the symmetry-adapted QP weights $Z_{+,-}$ (occupations $n_{+,-}$) which follow from diagonalizing the $\hat{Z}$ ($\hat{\Delta}^{(p)}$) matrix. Since Z_{12} is small in this case, the $Z_{+,-}$ are rather similar to $Z_{11}=Z_{22}$ and merge with the latter at half-filling. On the other hand, the polarization of the $(+,-)$ bands is still increasing.

As it is seen in Fig. 10 the off-diagonal component Z_{12} becomes increasingly important for larger U ($>U_c$) in the

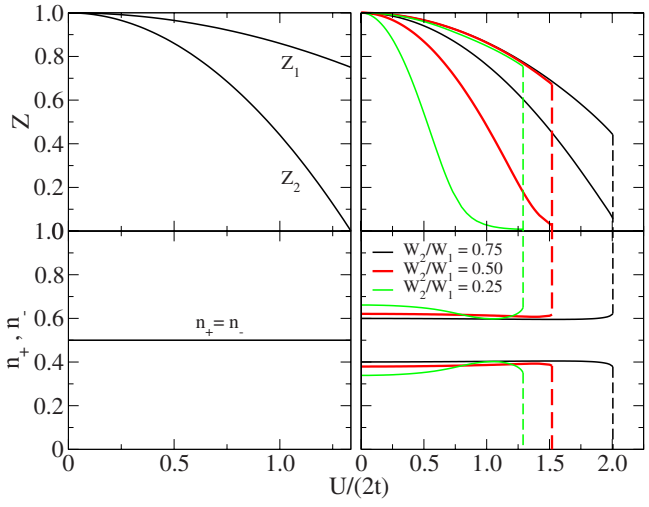

FIG. 8. (Color online) QP residues Z_i and symmetry-adapted fillings n_+, n_- for the half-filled bilayer. Left: $W_2/W_1=0.5$ and $V=0$. Right: various bandwidth ratios and $V=0.1$. In the right part, the curves for smaller Z and n are associated with the lower-bandwidth band.

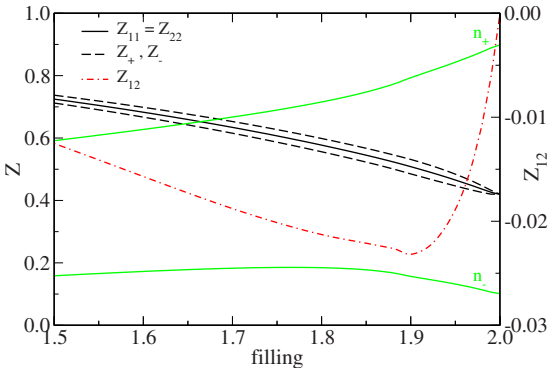

FIG. 9. (Color online) Doped bilayer with equal bandwidth and $V=0.25$ for $U=2.054$ ($<U_c$).

doped case. It follows that in this regime the QP weights $Z_{+,-}$ for the bonding and/or antibonding bands have rather different magnitudes and/or behaviors. Whereas Z_- is monotonically decreasing, Z_+ turns around and grows again (as also is the filling of the bonding band). Hence, this model is a simple example in which a differentiation between QP properties in different regions of the FS occur. Figure 11 shows the QP $(+,-)$ bands in the noninteracting and interacting cases ($U>U_c$), exhibiting strong orbital polarization and different band narrowing close to the insulating state. For very small doping and large U a transition to a new metallic phase is found, which will be discussed in detail in a forthcoming publication.[41]

Finally, we have also investigated a case in which the interlayer (interorbital) hopping does not have a local component ($V=0$), but does have a nonlocal one $V=t_{12}\neq 0$, treated in the band term of the Hamiltonian. Hence the corresponding energy matrix reads here

$$\varepsilon(\mathbf{k}) = -\frac{2}{3}\begin{pmatrix} t_{11} & t_{12} \\ t_{12} & t_{22} \end{pmatrix} \sum_{\mu=xyz} \cos(k_\mu a), \tag{63}$$

with the choice $t_{11}=t_{22}=0.5$ and $t_{12}=0.25$, as well as $a=1$. In that case, a continuous Mott transition within an OSMT sce-

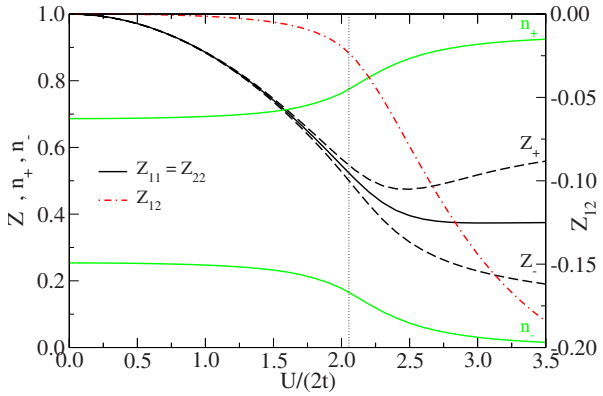

FIG. 10. (Color online) Bilayer at fixed doping ($n=1.88$) with equal bandwidth and $V=0.25$. Full green (gray) lines: fillings n_+, n_-; dashed dark lines: QP weights Z_+, Z_-. The vertical dotted line marks the critical U at half-filling.

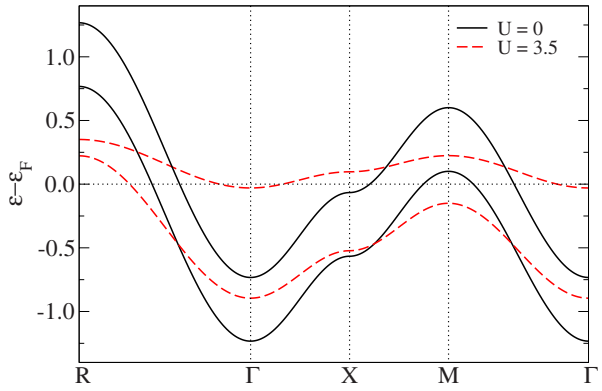

FIG. 11. (Color online) QP bands of the doped bilayer model ($n=1.88$) with equal bandwidths and $V=0.25$. The dominately filled band is the bonding one.

nario can be recovered, with, interestingly, a sizable value of the off-diagonal Z_{12} (Fig. 12). At the transition $Z_{11}=Z_{22}=Z_{12}\equiv Z_c$ holds, i.e., the $\hat{Z}$ matrix has a zero eigenvalue, associated with the (antibonding) insulating band. Note, however, that no net orbital polarization appears with V being purely nonlocal.

C. Application to the momentum dependence of the quasiparticle weight within cluster extensions of dynamical mean-field theory

In this section, we finally consider the implications of the rotationally invariant SB technique for the Mott transition and the momentum dependence of the QP weight, in the framework of cluster extensions of DMFT.

For simplicity, we consider a CDMFT approach to the two-dimensional Hubbard model with nearest-neighbor hopping t and a next-nearest neighbor hopping t', based on clusters consisting of two sites (dimers), arranged in a columnar way on the square lattice (see Fig. 13). The "local" Hamiltonian on each dimer is formally identical to the one introduced in the previous section for the bilayer model, i.e., Eq.

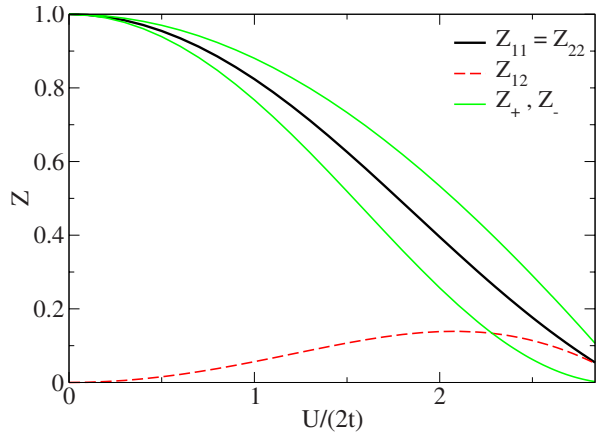

FIG. 12. (Color online) Half-filled bilayer, with equal bandwidths and $V=0$, but with a nonlocal interlayer hybridization t_{12}.

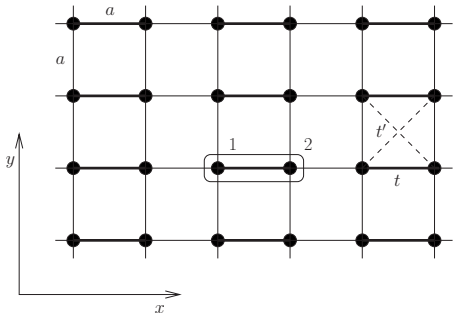

FIG. 13. Square lattice in the two-site CDMFT picture.

(62), with the value $V=-t$ of the "interorbital" hybridization. The interdimer kinetic-energy matrix reads (we set again $a=1$)

$$\varepsilon_{11}(\mathbf{K}) = \varepsilon_{22}(\mathbf{K}) = -2t\cos K_y,$$

$$\varepsilon_{12}(\mathbf{K}) = \varepsilon_{21}^{*}(\mathbf{K}) = -te^{i2K_x} - 2t'(1+e^{i2K_x})\cos K_y, \quad (64)$$

in which $\mathbf{K}$ denotes a momentum in the reduced Brillouin zone (BZ) of the superlattice: $K_x \in [-\pi/2, +\pi/2]$, $K_y \in [-\pi, +\pi]$. Note again that in SB calculations, the intradimer t has to be treated separately from the rest of the kinetic energy within H_{loc}. It is easy to check that when putting back $-t$ into the off-diagonal elements of the above kinetic-energy matrix, the eigenvalues just correspond to the one of a single band:

$$\varepsilon(\mathbf{k}) = -2t(\cos k_x + \cos k_y) - 4t' \cos k_x \cos k_y \quad (65)$$

in the full BZ of the original lattice $k_{x,y} \in [-\pi, +\pi]$. In the following, we set $t=0.25$ and consider successively $t'=0$ and $t'=-0.3t$ (a value appropriate to hole-doped cuprates). Note that, in this paper, we do not consider a bigger cluster than the two-site dimer, even in the presence of t'. Hence, the cluster self-energy will only contain Σ_{11} and Σ_{12} components, i.e., has a spatial range limited to the dimer. As a result, no renormalization of the effective t' is taken into account. This is of course an oversimplification (particularly in view of the demonstrated physical importance[11,12] of Σ_{13} close to the Mott transition). Larger clusters will be considered within the present SBMFT in a further publication. The goal of the present (simplified) study is to make a point of principle, namely, that the SB formalism can indeed produce a momentum-dependent $Z(\mathbf{k})$. As the cluster symmetry of the problem at hand is identical to the bilayer model from the last section, the number of nonzero SBs amounts again to 36. Figures 14–16 summarize the main findings, at half-filling and as a function of doping, respectively. Let us first concentrate on the case $t'=0$. Obviously, the Mott transition at half-filling in this case occurs in a manner which is very similar to the bilayer model with a finite interlayer hybridization studied in the previous section (Fig. 7): a *first-order* transition is found. The static part of the self-energy $\Sigma_{11}=\Sigma_{22}$ equals $U/2$, while Σ_{12} (which has no frequency dependence at half-filling within SBMFT) has a more complicated negative amplitude close to the transition. Note that we only discuss the paramagnetic solution, though, of course, the system

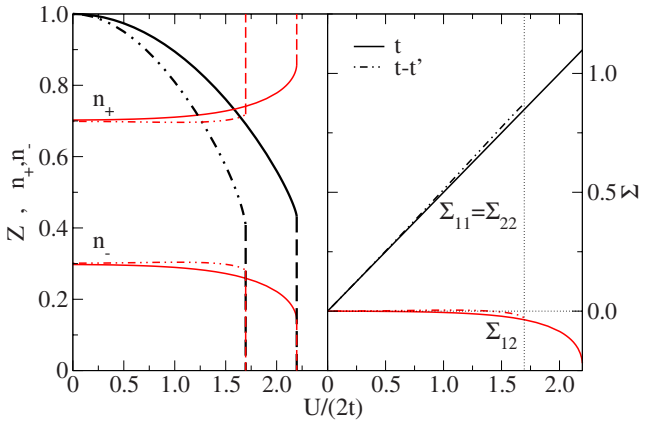

FIG. 14. (Color online) Half-filled two-dimensional Hubbard model within two-site CDMFT. Left: QP weights and band fillings; right: static dimer self-energy Σ.

is in principle unstable against antiferromagnetic order for any U. Upon doping, a finite value of Z_{12} is generated. The behavior of Z_{12} is rather similar to the case of the bilayer model, except for the change of sign (Figs. 15 and 16). Hence its amplitude is again significantly enhanced for $U > U_c$, i.e., the $Z_{+,-}$ values tend to manifestly deviate from each other. This is therefore signaling an increasingly nonlocal component of $Z(\mathbf{k})$ as the Mott insulating state is approached at strong coupling. Again, further studies in the latter regime at small doping will be published soon.[41]

Including the effect of a nonzero nearest-neighbor hopping $t' \neq 0$ turns out to lead to significant differences. Although the first-order character of the transition remains stable, the critical U is significantly lower (Fig. 14). The static components of the self-energy behave rather similarly to the t-only case, with some minor quantitative differences. There is a small negative Z_{12} with a maximum amplitude ~ 0.02, remaining nonzero also at the Mott transition (~ 0.01). The main difference in comparison to $t'=0$ is that here, in the doped case, Z_{12} changes sign from negative to positive close to the insulating regime for $U > U_c + \delta$ (with $\delta > 0$) (see Fig. 16). Thus the degree of correlation of the

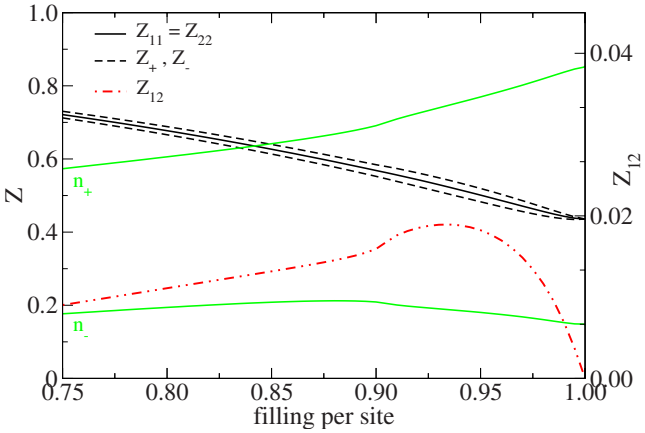

FIG. 15. (Color online) Doped two-dimensional Hubbard model ($t'=0$) within two-site CDMFT, for $U=2.195$ ($U_c \sim 2.197$).

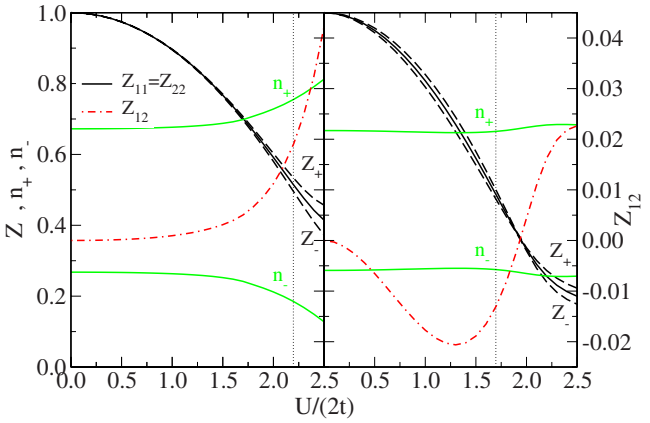

FIG. 16. (Color online) Two-dimensional Hubbard model within two-site CDMFT at fixed doping $n=0.94$. Left: t-only model; right: t-t' model ($t'=-0.3t$). The vertical lines denote the critical U at half-filling.

effective (bonding-antibonding) bands is inverted. These differences have to be interpreted with caution, since again the hopping range on the lattice is larger than our cluster size, and definitive conclusions will have to be drawn from a study involving Σ_{13} as well.

Nonetheless, keeping with the simplified treatment based on a two-site cluster, we now describe the resulting momentum dependence of the QP weight $Z(\mathbf{k})$ for the t-t' model. The matrix elements Σ_{11} and Σ_{12} of the cluster (physical) self-energy matrix Σ_c are obtained from the SB amplitudes at saddle point according to Eq. (55). The self-energy is then periodized on the whole lattice, in the form:[42,43]

$$\Sigma_{\text{lat}}(\mathbf{k},\omega) = \Sigma_{11}(\omega) + \tfrac{1}{2}\Sigma_{12}(\omega)(\cos k_x + \cos k_y). \quad (66)$$

The interacting FS is defined as follows:

$$\mu - \varepsilon(\mathbf{k}) - \Sigma_{\text{lat}}(\mathbf{k},\omega=0) = 0. \quad (67)$$

For our case, using Eqs. (65) and (66), this reads

$$\mu - \Sigma_{11}(0) + \left[2t - \tfrac{1}{2}\Sigma_{12}(0)\right](\cos k_x + \cos k_y) + 4t' \cos k_x \cos k_y = 0. \quad (68)$$

Hence the FS deforms in a nontrivial way in the presence of Σ_{lat}, when including t' in the present two-site CDMFT description. The QP weight $Z(\mathbf{k})$ can be derived from Σ_{lat} according to:

$$Z(\mathbf{k}) = \left[1 - \frac{\partial}{\partial\omega}\Sigma_{\text{lat}}(\mathbf{k},\omega)\right]^{-1}\Bigg|_{\mathbf{k}=\mathbf{k}_F}, \quad (69)$$

which leads here to

$$Z(\mathbf{k}) = \left[[\mathbf{Z}_\mathbf{c}^{-1}]_{11} + \tfrac{1}{2}[\mathbf{Z}_\mathbf{c}^{-1}]_{12}(\cos k_x + \cos k_y)\right]^{-1} = (Z_{11}^2 - Z_{12}^2)\left[Z_{11} - \tfrac{1}{2}Z_{12}(\cos k_x + \cos k_y)\right]^{-1}. \quad (70)$$

A contour plot of this function is displayed in Fig. 17. Note that it varies only according to $(\cos k_x + \cos k_y)$. Because the interacting FS involves both t and t', and hence both lattice harmonics $(\cos k_x + \cos k_y)$ and $\cos k_x \cos k_y$ (for $t' \neq 0$), it

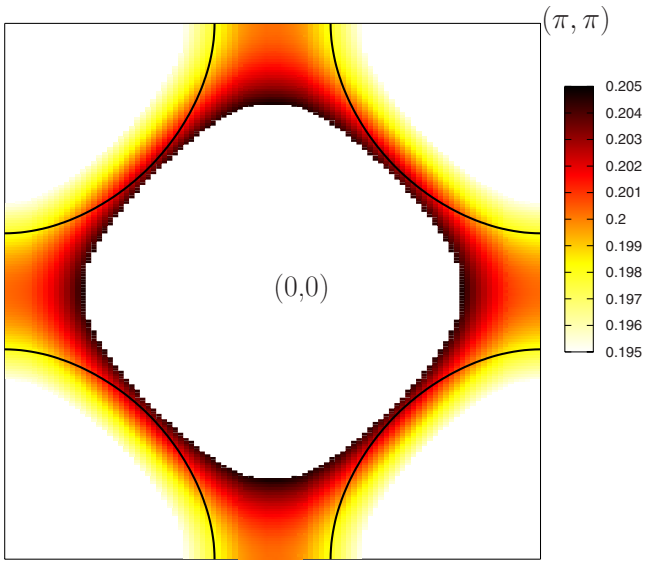

FIG. 17. (Color online) Interacting Fermi surface (solid lines) for the CDMFT treatment of the 2D t-t' Hubbard model with $t'=-0.3t$ and $U=2.5$ at $n=0.94$ (per site). The color contours show the variation of $Z(\mathbf{k})$ (smallest at antinodes).

cuts through different contour lines of $Z(\mathbf{k})$. This results in a QP weight which varies on the FS. Figure 17 shows $Z(\mathbf{k})$ for $\mathbf{k}$ close to the interacting FS. Albeit the momentum variation is quantitatively quite small, the key qualitative effect of Z being different on different parts of the FS is indeed found. It is seen that the QPs along the nodal direction, i.e., along (0,0)-(π,π), have slightly larger Z than the ones in the the antinodal direction $[(0,0)$-$(0,\pi)]$. Hence these results are indeed in qualitative agreement with ARPES measurements on cuprates. Note that to get nodal points to be more coherent that antinodal ones in this two-site scheme, $Z_{12}>0$ is actually crucial.

Our results provide an example of a SB calculation which can address the issue of the momentum dependence of the QP weight. We believe that the too small variation of Z along the FS found here is due to the oversimplified two-site description in which Σ_{13} is neglected. We intend to consider improvements on this issue using the present SBMFT in a forthcoming work.

Finally, let us make contact with previous work on the two-dimensional Hubbard model. Of course, this model has been intensively studied with a variety of methods such as: quantum Monte Carlo,[44,45] exact diagonalization,[46,47] path-integral renormalization group,[48] functional renormalization group,[49] and various quantum cluster methods (dynamical cluster approximation,[50] cluster extensions of dynamical mean-field theory,[7] and variational cluster perturbation theory[8]). We shall not attempt here a detailed comparison between the rotationally invariant SB method (which anyhow is a mean-field technique tailored to address low-energy issues) with the results of these numerical methods over the whole phase diagram (note, in particular, that we have not yet investigated long-range ordered phases, such as antiferromagnetism or superconductivity). Rather, we would like to point out that some recent numerical studies using the above methods[10–12,49] have indeed revealed the emergence of momentum-space differentiation in the two-dimensional Hubbard model. We hope that the rotationally invariant SB method will help us understand qualitatively the low-energy physics emerging from these results.

IV. CONCLUSION AND PERSPECTIVES

In this paper, we extended and generalized the rotationally invariant formulation of the slave-boson method.[13,14]

Our formulation achieves two goals: (i) extending the slave-boson method in order to accommodate the most general crystal fields, interactions, and multiplet structures and (ii) the development of a technique which can describe QP weights and Fermi liquid parameters which vary along the Fermi surface.

The key aspect of the formalism is to introduce slave-boson fields which form a matrix with entries labeled by a pair of a physical state and a QP state (within an arbitrary choice of basis set). As a result, a density matrix is constructed instead of just a probability amplitude for each state.

While the first objective (i) could also be achieved by generalizing appropriately the Gutzwiller approximation,[15,16] we find the slave-boson approach to be somewhat more flexible, in the sense that it is a mean-field theory which can in principle be improved by computing fluctuations around the saddle point. Our application to the two-band model seems promising. While further work is needed to benchmark the accuracy of the rotationally invariant slave-boson method against exact quantum impurity solvers, it is clear that already in the single site multiorbital DMFT setting, our method has numerous advantages. It obeys the Luttinger theorem even in the presence of multiplets, and can accommodate full atomic physics information. Furthermore, the off-diagonal elements of the matrix of QP weights can be calculated within this method, while the standard slave-boson or Gutzwiller approximations (using probability amplitudes instead of a density matrix) cannot achieve this goal.

Our technique achieves the second objective (ii) via a detour, namely, the use of cluster extensions of dynamical mean-field theory in order to reduce the lattice to a multisite (molecular) impurity problem, to which we apply our rotationally invariant slave-boson method as an impurity solver. Because the intersite matrix elements of the QP weight can be calculated, it leads on the lattice to a momentum dependence of the QP residue $Z(\mathbf{k})$. We successfully demonstrated this point, in the framework of a two-site CDMFT study of the single-band 2D Hubbard model. We did find that the QP weight at the nodes is somewhat larger than at the antinodes, although the magnitude of this effect is expected to increase within a more realistic study involving a larger cluster (e.g., a square plaquette), which is left for future work. A major challenge is the direct extension of our slave-boson approach to the lattice, without resorting to the cluster-DMFT detour. In this context, we mention that other slave-boson techniques, which introduce magnetic correlations through the use of link variables to decouple the superexchange J term,[1] can be interpreted in terms of a $\mathbf{k}$-dependent self-energy. However, within such schemes, the derivative of the self-

energy with respect to frequency is momentum *independent* (in contrast to the static part), yielding a **k**-independent QP residue. Hence, our approach goes beyond these methods, at least in conjunction with the cluster-DMFT approach. We hope that having an economic impurity solver based on SBs will allow us to study larger cluster sizes than feasible with other methods, and most importantly help us understand the low-energy physics emerging from these cluster dynamical mean-field theories.

Finally, we limited our study to slave bosons which do not mix the particle number. The extension to full charge-rotational invariance and superconductivity is possible (see Refs. 14 and 22 in the single-orbital case), and will be presented in a separate paper. In this context, the slave-boson method will incorporate the SU(2) charge symmetry and its extension away from half-filling considered by Wen and Lee[51] and the rotationally invariant slave-boson formalism can serve as a powerful tool for interpreting the low-energy physics emerging from plaquette-CDMFT studies of this issue.

ACKNOWLEDGMENTS

We are grateful to Pablo Cornaglia and Michel Ferrero for very useful discussions and remarks. As this work was being completed, we learned of a parallel effort by Michele Fabrizio (Ref. 52), in the framework of the Gutzwiller approximation. In particular, the form of the constraints advocated in this work matches our constraints (28) and (29) in SB language. A.G. also thanks him for discussions. This work has been supported by the "Chaire Blaise Pascal" (région Ile de France and Fondation de l'Ecole Normale Supérieure), the European Union (under contract "Psi-k f-electrons" HPRN-CT-2002-00295), the CNRS, and Ecole Polytechnique. G.K. was supported by the NSF under Grant No. DMR 0528969.

APPENDIX A: SINGLE-ORBITAL CASE AND CONNECTION WITH PREVIOUS WORK

Here, we briefly consider the single-orbital case ($M=2$), which also allows us to make contact with Refs. 13 and 14. These authors introduced in this case a rotationally invariant formalism, with the calculation of response functions associated with the saddle point as their main motivation. For $M=2$, the following local basis set can be considered (whether or not H_{loc} is diagonal in this basis):

$$N=0:\ |0\rangle,$$

$$N=1:\ |\sigma\rangle = d_\sigma^\dagger|0\rangle,$$

$$N=2:\ |D\rangle = d_\uparrow^\dagger d_\downarrow^\dagger|0\rangle. \tag{A1}$$

Hence, we introduce the following bosons (not mixing sectors with different particle numbers, i.e., not considering superconducting states):

$$\phi_{00}\equiv\phi_E,\quad \phi_{\sigma\sigma'},\quad \phi_{\uparrow\downarrow}\equiv\phi_D. \tag{A2}$$

Up to normalizations, the bosons $p_{\sigma\sigma'}^\dagger$ introduced in Ref. 13 correspond to $\phi_{\sigma\sigma'}^\dagger$. In contrast, the standard Kotliar-Ruckenstein[17] formalism introduces only *two* bosons $p_\sigma^\dagger$ in the one-particle sector. The representatives (27) of the physical states read here

$$|\underline{0}\rangle = \phi_E^\dagger|\mathrm{vac}\rangle,$$

$$|\underline{\sigma}\rangle = \frac{1}{\sqrt{2}}\sum_{\sigma'}\phi_{\sigma\sigma'}^\dagger f_{\sigma'}^\dagger|\mathrm{vac}\rangle,$$

$$|\underline{D}\rangle = \phi_D^\dagger d_\uparrow^\dagger d_\downarrow^\dagger|\mathrm{vac}\rangle, \tag{A3}$$

and the constraints (28) and (29) read

$$1 = \phi_E^\dagger\phi_E + \sum_{\sigma\sigma'}\phi_{\sigma\sigma'}^\dagger\phi_{\sigma\sigma'} + \phi_D^\dagger\phi_D, \tag{A4}$$

$$f_\alpha^\dagger f_\alpha = \phi_D^\dagger\phi_D + \sum_\sigma \phi_{\sigma\alpha}^\dagger\phi_{\sigma\alpha}, \tag{A5}$$

$$f_\uparrow^\dagger f_\downarrow = \sum_\sigma \phi_{\sigma\downarrow}^\dagger\phi_{\sigma\uparrow}, \tag{A6}$$

$$f_\downarrow^\dagger f_\uparrow = \sum_\sigma \phi_{\sigma\uparrow}^\dagger\phi_{\sigma\downarrow}. \tag{A7}$$

Not including, for simplicity, the square-root normalizations in Eq. (37), needed in order to ensure a correct $U=0$ limit at saddle point, the "simplest" expression (32) of the electron creation operators reads

$$\underline{d}_\uparrow^\dagger = \frac{1}{\sqrt{2}}\sum_\beta[\phi_{\uparrow\beta}^\dagger\phi_E + (-1)^\beta\phi_D^\dagger\phi_{\downarrow\bar{\beta}}]f_\beta^\dagger, \tag{A8}$$

$$\underline{d}_\downarrow^\dagger = \frac{1}{\sqrt{2}}\sum_\beta[\phi_{\downarrow\beta}^\dagger\phi_E - (-1)^\beta\phi_D^\dagger\phi_{\uparrow\bar{\beta}}]f_\beta^\dagger. \tag{A9}$$

Apart from the motivations of Ref. 13 (associated with fluctuations and response functions), the usefulness of the rotationally invariant scheme in the single-orbital case can be demonstrated on a toy model consisting of a one-band Hubbard model with a magnetic field, purposely written in the S^x direction (i.e., in the form $hd_\uparrow^\dagger d_\downarrow$+h.c., analogous to a hybridization). Although the direction of the field should not matter, a direct application of the standard Kotliar-Ruckenstein formalism is impossible in that case. The rotationally invariant formalism can be shown to lead to the correct saddle point, independently of the spin-quantization axis.

APPENDIX B: DERIVATION OF EQUATION (29)

In this section, we show that the physical states of the form (27) are exactly those selected by the constraints (28) and (29). First, it is easy to check that states of the form (27) do satisfy these constraints. Indeed, let us act on the state $|\underline{C}\rangle \equiv \frac{1}{\sqrt{D_C}}\Sigma_m\phi_{Cm}^\dagger|\mathrm{vac}\rangle\otimes|m\rangle_f$ and with Eq. (29). The left-hand side (lhs) leads to

$$f_\alpha^\dagger f_{\alpha'}|\underline{C}\rangle = \frac{1}{\sqrt{D_C}}\sum_m \phi_{Cm}^\dagger|\mathrm{vac}\rangle \otimes f_\alpha^\dagger f_{\alpha'}|m\rangle_f$$
$$= \frac{1}{\sqrt{D_C}}\sum_{mm'} \langle m'|f_\alpha^\dagger f_{\alpha'}|m\rangle \phi_{Cm}^\dagger|\mathrm{vac}\rangle \otimes |m'\rangle_f. \tag{B1}$$

When acting with the rhs, only the terms $A=C$ and $n=m$ give a nonvanishing contribution. Hence,

$$\sum_A \sum_{nn'} \phi_{An'}^\dagger \phi_{An}\langle n|f_\alpha^\dagger f_{\alpha'}|n'\rangle|\underline{C}\rangle$$
$$= \frac{1}{\sqrt{D_C}}\sum_{nn'} \langle n|f_\alpha^\dagger f_{\alpha'}|n'\rangle \phi_{Cn'}^\dagger|\mathrm{vac}\rangle \otimes |n\rangle_f.$$

We now prove that Eq. (29) is a *sufficient* condition, which is a bit more difficult. Since Eq. (28) excludes states with more than one boson, it is enough to consider a general state of the form

$$|C;W\rangle \equiv \sum_{pq} W_{pq}\phi_{Cp}^\dagger|\mathrm{vac}\rangle \otimes |q\rangle_f, \tag{B2}$$

and to show that Eq. (29) implies $W_{pq} \propto \delta_{pq}$. Acting on this state with each term in the constraint (29) yields for the lhs

$$f_\alpha^\dagger f_{\alpha'}|C;W\rangle = \sum_{pq} W_{pq}\phi_{Cp}^\dagger|\mathrm{vac}\rangle \otimes f_\alpha^\dagger f_{\alpha'}|q\rangle_f$$
$$= \sum_{pr} \phi_{Cp}^\dagger|\mathrm{vac}\rangle \otimes |r\rangle_f \sum_q W_{pq}\langle r|f_\alpha^\dagger f_{\alpha'}|q\rangle. \tag{B3}$$

Let us now act with the rhs. Only the terms with $A=C$ and $n=p$ contribute, leading to

$$\sum_A \sum_{nn'} \phi_{An'}^\dagger \phi_{An}\langle n|f_\alpha^\dagger f_{\alpha'}|n'\rangle|C;W\rangle$$
$$= \sum_{pqn'} W_{pq}\phi_{Cn'}^\dagger|\mathrm{vac}\rangle \otimes |q\rangle_f\langle p|f_\alpha^\dagger f_{\alpha'}|n'\rangle$$
$$= \sum_{pr} \phi_{Cp}^\dagger|\mathrm{vac}\rangle \otimes |r\rangle_f \sum_q W_{qr}\langle q|f_\alpha^\dagger f_{\alpha'}|p\rangle, \tag{B4}$$

where the last expression comes from a change of indices $n' \to p$, $q \to r$, and $p \to q$.

We see that the constraint is satisfied provided that the following identity holds, *for all orbital indices* $\alpha\alpha'$ *and all* states p, r:

$$\sum_q W_{pq}\langle r|f_\alpha^\dagger f_{\alpha'}|q\rangle = \sum_q W_{qr}\langle q|f_\alpha^\dagger f_{\alpha'}|p\rangle. \tag{B5}$$

Let us first look at the case $\alpha=\alpha'$, which reads

$$r_\alpha W_{pr} = p_\alpha W_{pr}. \tag{B6}$$

Hence $W_{pr}=0$ unless $p_\alpha=r_\alpha$ for all α, so that

$$W_{pq} = w_p\delta_{pq}. \tag{B7}$$

Substituting this into Eq. (B5), we obtain

$$w_p\langle r|f_\alpha^\dagger f_{\alpha'}|p\rangle = w_r\langle r|f_\alpha^\dagger f_{\alpha'}|p\rangle. \tag{B8}$$

Thus, if r and p are related by a move of a QP from one state to another (a transposition of two occupation numbers), then $w_p=w_r$. Moreover, two Fock states in the same sector H_N of the Hilbert space are related by a permutation of the occupied states, which can be decomposed in a product of transpositions. Hence, w_p is a constant for $p \in H_N$, and $W_{pq} \propto \delta_{pq}$ as claimed.

APPENDIX C: PHYSICAL CREATION OPERATOR

1. Proximate expression

First let us note that there is a systematic route to find the expression for d, which consists in writing the operator as

$$\underline{d}_\alpha^\dagger = \sum_{AB}\langle A|d_\alpha^\dagger|B\rangle|\underline{A}\rangle\langle\underline{B}| = \sum_{AB}\sum_{n\in H_A, m\in H_B}\langle A|d_\alpha^\dagger|B\rangle\phi_{An}^\dagger\phi_{Bm}X_{nm}^f, \tag{C1}$$

with $X_{nm}^f=|n\rangle_f\langle m|_f$ in usual Hubbard notations. X_{nm}^f is obviously *not* just a one-particle operator $f^\dagger$, even when restricted to the sectors of interest in the above formula, since the states n and m can differ in many places. However, because any transposition of two QPs, *when acting on a physical state*, can be replaced by a corresponding operation on bosons using the constraint (29), and because any product of bosonic operators which cannot be reduced to a quadratic form will produce a state which is out of the physical subspace, the physical operator *must* in the end take the form

$$\underline{d}_\alpha^\dagger = \sum_\beta \sum_{AB} \sum_{nm} C_{Bm}^{An}(\alpha,\beta)\phi_{An}^\dagger\phi_{Bm}f_\beta^\dagger. \tag{C2}$$

One can solve for the coefficients $C_{Bm}^{An}(\alpha,\beta)$, requesting proper action on the physical states.

In this section, however, we restrict ourselves to proving that Eq. (32) does the job, i.e., that

$$\underline{d}_\alpha^\dagger = \sum_{\beta,AB,nm} \frac{\langle A|d_\alpha^\dagger|B\rangle\langle n|f_\beta^\dagger|m\rangle}{\sqrt{N_A(M-N_B)}}\phi_{An}^\dagger\phi_{Bm}f_\beta^\dagger \tag{C3}$$

satisfies

$$\underline{d}_\alpha^\dagger|\underline{B}\rangle = \sum_A \langle A|d_\alpha^\dagger|B\rangle|\underline{A}\rangle. \tag{C4}$$

We start by proving the formula

$$\sum_\beta \sum_{p\in H_N} \langle n|f_\beta^\dagger|p\rangle f_\beta^\dagger|p\rangle = (N+1)|n\rangle, \tag{C5}$$

where the sum over p runs over the basis of the subspace H_N (states with N QPs) of the Fock space. First, we have in general

$$\sum_\beta \sum_{p\in H_N} \langle n|f_\beta^\dagger|p\rangle f_\beta^\dagger|p\rangle = \sum_{n'\in H_{N+1}} a_{n'}|n'\rangle, \tag{C6}$$

but, because $f^\dagger$ is the creation operator (it connects one basis state to only one another),

$$a_{n'} = \sum_{\beta,p\in H_N} \langle n|f_\beta^\dagger|p\rangle\langle n'|f_\beta^\dagger|p\rangle \propto \delta_{nn'} \sum_{\beta,p\in H_N} |\langle n|f_\beta^\dagger|p\rangle|^2. \tag{C7}$$

We now use the fact that the tensor is invariant (it has the same expression in every basis) and use the notations introduced for Eq. (40): U is a unitary transformation of the one QP states and $\mathcal{U}$ is the corresponding transformation in the Fock states. $\langle n|f_\beta^\dagger|m\rangle = U_{\beta\beta'}\mathcal{U}^*_{nn'}\langle n'|f_{\beta'}^\dagger|m'\rangle\mathcal{U}_{mm'}$ and we have

Moreover, any couple of elements of the basis of the Fock state can be connected by a $\mathcal{U}$ transformation (with a U that permutes the one QP basis state); therefore, $a_n \equiv a$ is independent of n. a can then be determined by summing Eq. (C5) over n,

$$\sum_{n\in H_{N+1}} a_n = \sum_\beta \sum_{\substack{n\in H_{N+1}\\ p\in H_N}} |\langle n|f_\beta^\dagger|p\rangle|^2 = \sum_{n\in H_{N+1}} \langle n|\sum_\beta f_\beta^\dagger f_\beta|n\rangle$$

$$= \sum_{n\in H_{N+1}} (N+1), \tag{C9}$$

leading to $a=N+1$. This completes the proof of Eq. (C5).

It is now simple to compute the action of Eq. (32): acting on $|\underline{C}\rangle \equiv \frac{1}{\sqrt{D_C}}\Sigma_p \phi_{Cp}^\dagger|\text{vac}\rangle\otimes|p\rangle_f$ with this operator, only the term $B=C$, $m=p$ contributes, and we get

$$\underline{d}_\alpha^\dagger|\underline{C}\rangle = \frac{1}{\sqrt{D_C(N_C+1)(M-N_C)}} \sum_{A,n\in H_{N_C+1}} \langle A|d_\alpha^\dagger|C\rangle\phi_{An}^\dagger|\text{vac}\rangle$$
$$\otimes \sum_\beta \sum_{p\in H_{N_C}} \langle n|f_\beta^\dagger|p\rangle f_\beta^\dagger|p\rangle$$
$$= \sqrt{\frac{N_C+1}{D_C(M-N_C)}} \sum_{A,n\in H_{N_C+1}} \langle A|d_\alpha^\dagger|C\rangle\phi_{An}^\dagger|\text{vac}\rangle\otimes|n\rangle$$
$$= \sum_A \langle A|d_\alpha^\dagger|C\rangle|\underline{C}\rangle, \tag{C10}$$

which is identical to Eq. (31).

2. Improved expression

In this section we present arguments for the improved formula used in this paper. First, it is useful to define the "natural orbital" (NO) basis as the basis which diagonalizes the quasiparticle and quasihole density matrices corresponding to the average constraint, which is given by

$$\hat{\Delta}^{(p)}_{\alpha\beta}[\phi] \equiv \sum_{Anm} \phi^*_{An}\phi_{Am}\langle m|f_\alpha^\dagger f_\beta|n\rangle, \tag{C11a}$$

$$\hat{\Delta}^{(h)}_{\alpha\beta}[\phi] \equiv \sum_{Anm} \phi^*_{An}\phi_{Am}\langle m|f_\beta f_\alpha^\dagger|n\rangle = \sum_{An} \phi^*_{An}\phi_{An} - \hat{\Delta}^{(p)}_{\alpha\beta}[\phi]. \tag{C11b}$$

Let us denote by ξ_λ, $|\lambda\rangle$ the eigenvalues and eigenvectors of those matrices:

$$\hat{\Delta}^{(p)}_{\alpha\beta} = \sum_\lambda \xi_\lambda\langle\alpha|\lambda\rangle\langle\lambda|\beta\rangle, \quad |\lambda\rangle = \sum_\lambda \langle\alpha|\lambda\rangle|\alpha\rangle, \tag{C12}$$

which is equivalent to use the NO quasiparticle operator $\psi_\lambda^\dagger$ such that

$$\psi_\lambda^\dagger \equiv \sum_\alpha \langle\lambda|\alpha\rangle f_\alpha^\dagger, \quad \langle\psi_\lambda^\dagger\psi_\mu\rangle = \delta_{\lambda\mu}\xi_\lambda. \tag{C13}$$

To be fully explicit, we can consider the particular basis transformation (in the notations of the section above) $f_\alpha^\dagger = U_{\alpha\lambda}\psi_\lambda^\dagger$ which rotates to the NOs, and the corresponding rotation on the bosons: $\phi_{An} = \mathcal{U}(U)_{nn'}\Omega_{An'}$. The rotation matrix is

$$U_{\alpha\lambda} = \langle\alpha|\lambda\rangle, \tag{C14}$$

and in the NO basis,

$$\sum_{Anm} \Omega^*_{An}\Omega_{Bm}\langle m|\psi_\lambda^\dagger\psi_\mu|n\rangle = \delta_{\lambda\mu}\sum_{An} \Omega^*_{An}\Omega_{An}n_\lambda = \delta_{\lambda\mu}\xi_\lambda(\{\Omega_{An}\}), \tag{C15}$$

and

$$\hat{\Delta}^{(p)}_{\alpha\beta}[\phi] = \sum_\lambda U_{\alpha\lambda}\xi_\lambda[U^\dagger]_{\lambda\beta}. \tag{C16}$$

The idea is to generalize the Kotliar-Ruckenstein normalization factor in the NO basis, where the QP density being diagonal, its probabilistic interpretation is more transparent. Hence, the improved expression of d reads

$$\underline{d}_\alpha^\dagger = \sum_{\lambda,AB,nm} \frac{\langle A|d_\alpha^\dagger|B\rangle\langle n|\psi_\lambda^\dagger|m\rangle}{\sqrt{\xi_\lambda(\{\Omega_{An}\})(1-\xi_\lambda(\{\Omega_{An}\}))}}\Omega_{An}^\dagger\Omega_{Bm}\psi_\lambda^\dagger. \tag{C17}$$

Note that the formal square-root normalization, i.e., $1/\sqrt{N_A(M-N_B)}$, does not appear in this representation. We can now rotate back to the generic basis we started from and use the gauge invariance, leading to

$$\underline{d}_\alpha^\dagger = \sum_{AB,nm,\beta\gamma} \mathcal{C}^{An}_{Bm}(\alpha,\beta)\phi_{An}^\dagger\phi_{Bm}\sum_\lambda \frac{\langle\beta|\lambda\rangle\langle\lambda|\gamma\rangle}{\sqrt{\xi_\lambda(1-\xi_\lambda)}}f_\gamma^\dagger$$
$$= \sum_{AB,nm,\beta\gamma} \mathcal{C}^{An}_{Bm}(\alpha,\beta)\phi_{An}^\dagger\phi_{Bm}\langle\beta|[\hat{\Delta}^{(p)}\hat{\Delta}^{(h)}]^{-1/2}|\gamma\rangle f_\gamma^\dagger \tag{C18}$$

with

$$\mathcal{C}^{An}_{Bm}(\alpha,\beta) = \langle A|d_\alpha^\dagger|B\rangle\langle n|f_\beta^\dagger|m\rangle. \tag{C19}$$

Hence this yields the following form for the R matrix:

$$R[\phi]^*_{\alpha\beta} = \sum_{AB,nm,\delta} \mathcal{C}^{An}_{Bm}(\alpha,\delta)\phi_{An}^\dagger\phi_{Bm}\langle\delta|[\hat{\Delta}^{(p)}\hat{\Delta}^{(h)}]^{-1/2}|\beta\rangle. \tag{C20}$$

In the actual implementation of the saddle-point calculations, the explicit use of both the quasiparticle and the quasihole density matrices has been utilized (i.e., *not using their relation*). Although *at convergence* the different representations yield the same values, writing the equations via both

particle and hole density matrix appears to be necessary within the minimization cycle. This is due to the fact that the derivatives with respect to the slave bosons have to be symmetric, however, when using only the particle density matrix (or its eigensystem decomposition) for instance, the derivative with respect to the empty boson vanish, although this one exists in the Kotliar-Ruckenstein case. In the end an even more symmetrized form, i.e., $\frac{1}{2}(\hat{\Delta}^{(p)}\hat{\Delta}^{(h)}+\hat{\Delta}^{(h)}\hat{\Delta}^{(p)})$ was used for the square root in Eq. (C18). Thus defining the following matrix:

$$M_{\gamma\beta}=\left\langle \gamma\left|\left[\tfrac{1}{2}(\hat{\Delta}^{(p)}\hat{\Delta}^{(h)}+\hat{\Delta}^{(h)}\hat{\Delta}^{(p)})\right]^{-1/2}\right|\beta\right\rangle, \tag{C21}$$

the electron operators are written as

$$d_\alpha^\dagger=\sum_{AB}\sum_{nm}\sum_{\gamma\beta}\mathcal{C}_{Bm}^{An}(\alpha,\gamma)\phi_{An}^\dagger\phi_{Bm}M_{\gamma\beta}f_\beta^\dagger=\sum_\beta R_{\alpha\beta}^*f_\beta^\dagger, \tag{C22}$$

$$d_\alpha=\sum_{AB}\sum_{nm}\sum_{\gamma\beta}\mathcal{C}_{Bm}^{An}(\alpha,\gamma)\phi_{Bm}^\dagger\phi_{An}M_{\beta\gamma}f_\beta=\sum_\beta R_{\alpha\beta}f_\beta, \tag{C23}$$

and correspondingly independently written the elements of the R, $R^\dagger$ matrices read

$$R[\phi]_{\alpha\beta}=\sum_{AB,nm,\gamma}\mathcal{C}_{Bm}^{An}(\alpha,\gamma)\phi_{Bm}^\dagger\phi_{An}\hat{M}_{\beta\gamma}, \tag{C24}$$

$$R^\dagger[\phi]_{\alpha\beta}\equiv R[\phi]_{\beta\alpha}^*=\sum_{AB,nm,\gamma}\mathcal{C}_{Bm}^{An}(\beta,\gamma)\phi_{An}^\dagger\phi_{Bm}\hat{M}_{\gamma\alpha}. \tag{C25}$$

APPENDIX D: DETAILS ON THE SADDLE-POINT EQUATIONS AND THEIR NUMERICAL SOLUTION

The saddle-point equations for $T=0$ are obtained by performing the partial derivatives with respect to all the variables, i.e., condensed slave-boson amplitudes and Lagrange multipliers as follows:

$$\frac{\partial\Omega}{\partial\lambda_0}=1-\sum_{An}\varphi_{An}^\dagger\varphi_{An}, \tag{D1}$$

$$\frac{\partial\Omega}{\partial\Lambda_{\alpha\beta}}=\langle f_\alpha^\dagger f_\beta\rangle-\sum_{A,nn'}\varphi_{An'}^\dagger\langle n|d_\alpha^\dagger d_\beta|n'\rangle\varphi_{An}, \tag{D2}$$

$$\frac{\partial\Omega}{\partial\varphi_{Cm}}=\sum_{\mathbf{k}j}\tilde{f}_{\mathbf{k}j}\frac{\partial\varepsilon_{\mathbf{k}j}}{\partial\varphi_{Cm}}+\sum_A E_{AC}\varphi_{Am}^\dagger+\lambda_0\varphi_{Cm}^\dagger-\sum_{\alpha\beta}\Lambda_{\alpha\beta}\sum_{n'}\langle m|d_\alpha^\dagger d_\beta|n'\rangle\varphi_{Cn'}^\dagger, \tag{D3}$$

$$\frac{\partial\Omega}{\partial\varphi_{Cm}^\dagger}=\sum_{\mathbf{k}j}\tilde{f}_{\mathbf{k}j}\frac{\partial\varepsilon_{\mathbf{k}j}}{\partial\varphi_{Cm}^\dagger}+\sum_B E_{CB}\varphi_{Bm}^\dagger+\lambda_0\varphi_{Cm}-\sum_{\alpha\beta}\Lambda_{\alpha\beta}\sum_n\langle n|d_\alpha^\dagger d_\beta|m\rangle\varphi_{Cn} \tag{D4}$$

with

$$\langle f_\alpha^\dagger f_\beta\rangle=\sum_{\mathbf{k}j}\tilde{f}_{\mathbf{k}j}\langle\alpha|\nu_{\mathbf{k}j}\rangle\langle\nu_{\mathbf{k}j}|\beta\rangle. \tag{D5}$$

The $\varepsilon_{\mathbf{k}j}$ are the eigenvalues (with band index j) of the QP matrix $(\mathbf{R}^\dagger(\varphi)\boldsymbol{\varepsilon}(\mathbf{k})\mathbf{R}(\varphi)+\boldsymbol{\Lambda})$ with corresponding eigenvector $|\nu_{\mathbf{k}j}\rangle$, while $\tilde{f}_{\mathbf{k}j}$ denotes the occupation number of the state $|\nu_{\mathbf{k}j}\rangle$ for a given total number of particles, to be evaluated by standard k-integration techniques (e.g., tetrahedron method, Gaussian smearing, etc.).

1. Some slave-boson derivatives

(*a*) *Eigenvalues and R matrices*. The derivatives of the eigenvalues with respect to the slave bosons, i.e., $\frac{\partial\varepsilon_{\mathbf{k}j}}{\partial\varphi}$, may be performed pertubatively as follows:

$$\begin{aligned}\frac{\partial\varepsilon_{\mathbf{k}j}}{\partial\varphi}&=\left\langle\nu_{\mathbf{k}j}\left|\frac{\partial}{\partial\varphi}(\mathbf{R}^\dagger\boldsymbol{\varepsilon}(\mathbf{k})\mathbf{R}+\Lambda)\right|\nu_{\mathbf{k}j}\right\rangle\\&=\left\langle\nu_{\mathbf{k}j}\left|\frac{\partial\mathbf{R}^\dagger}{\partial\varphi}\boldsymbol{\varepsilon}(\mathbf{k})\mathbf{R}+\mathbf{R}^\dagger\boldsymbol{\varepsilon}(\mathbf{k})\frac{\partial\mathbf{R}}{\partial\varphi}\right|\nu_{\mathbf{k}j}\right\rangle\\&=\left\langle\nu_{\mathbf{k}j}\left|\sum_{\alpha\beta}|\alpha\rangle\frac{\partial\hat{R}_{\alpha\beta}^\dagger}{\partial\varphi}\langle\beta|\boldsymbol{\varepsilon}(\mathbf{k})\mathbf{R}\right.\right.\\&\quad\left.\left.+\sum_{\alpha\beta}\mathbf{R}^\dagger\boldsymbol{\varepsilon}(k)|\alpha\rangle\frac{\partial\hat{R}_{\alpha\beta}}{\partial\varphi}\langle\beta\,|\nu_{\mathbf{k}j}\rangle\right.\right.\\&=\sum_{\alpha\beta}\left[\langle\nu_{\mathbf{k}j}|\alpha\rangle\frac{\partial\hat{R}_{\alpha\beta}^\dagger}{\partial\varphi}\langle\beta|\boldsymbol{\varepsilon}(\mathbf{k})\mathbf{R}|\nu_{\mathbf{k}j}\rangle\right.\\&\quad\left.+\langle\nu_{\mathbf{k}j}|\mathbf{R}^\dagger\boldsymbol{\varepsilon}(\mathbf{k})|\alpha\rangle\frac{\partial\hat{R}_{\alpha\beta}}{\partial\varphi}\langle\beta|\nu_{\mathbf{k}j}\rangle\right].\end{aligned} \tag{D6}$$

The therefore needed explicit expressions for the derivatives of the R, $R^\dagger$ matrices read as follows [using Eqs. (C24) and (C25)]:

$$\frac{\partial\hat{R}_{\alpha\beta}}{\partial\varphi_{Cm}}=\sum_{AB,nn',\gamma}\mathcal{C}_{Bn'}^{An}(\alpha,\gamma)\varphi_{Bn'}^\dagger\left(\delta_{An}^{Cm}\hat{M}_{\beta\gamma}+\varphi_{An}\frac{\partial\hat{M}_{\beta\gamma}}{\partial\varphi_{Cm}}\right),$$

$$\frac{\partial\hat{R}_{\alpha\beta}}{\partial\varphi_{Cm}^\dagger}=\sum_{AB,nn',\gamma}\mathcal{C}_{Bn'}^{An}(\alpha,\gamma)\varphi_{An}\left(\delta_{Bn'}^{Cm}\hat{M}_{\beta\gamma}+\varphi_{Bn'}^\dagger\frac{\partial\hat{M}_{\beta\gamma}}{\partial\varphi_{Cm}^\dagger}\right)\quad\text{(analogous for }[\hat{R}^\dagger]_{\alpha\beta}).$$

(*b*) *The* **M** *matrix*. As it is seen, the derivatives involve the derivative of the **M** matrix (C21). This derivative is computed as follows. Let us first write **M** as

$$\hat{M}_{\gamma\beta} = \langle \gamma | \mathbf{K}^{-1/2} | \beta \rangle. \tag{D7}$$

What we are looking for is the derivative of $\mathbf{K}^{-1/2}$ with respect to the SBs. In order to get access to this quantity we use the identity

$$(\partial_\varphi \mathbf{K}^{-1/2})\mathbf{K}^{-1/2} + \mathbf{K}^{-1/2}(\partial_\varphi \mathbf{K}^{-1/2}) = \partial_\varphi \mathbf{K}^{-1} \tag{D8}$$

$$\Leftrightarrow \mathbf{X}\mathbf{K}^{-1/2} + \mathbf{K}^{-1/2}\mathbf{X} = \mathbf{Y}, \tag{D9}$$

with $\mathbf{X} = \partial_\varphi \mathbf{K}^{-1/2}$ and $\mathbf{Y} = \partial_\varphi \mathbf{K}^{-1}$. We then apply $\mathbf{P}$ which transforms $\mathbf{K}$ to its eigensystem. This yields

$$\mathbf{X}'\mathbf{L} + \mathbf{L}\mathbf{X}' = \mathbf{Y}', \tag{D10}$$

where the prime denotes that the quantities defined above are expressed in that eigensystem, and $\mathbf{L} = \mathbf{P}^\dagger \mathbf{K}^{-1/2} \mathbf{P}$. Since in the eigensystem $\mathbf{K}^{-1/2}$ is diagonal, i.e., $\mathbf{L}$ is, the last equation can be written in components and $\mathbf{X}'$ determined as follows:

$$X'_{ij}L_j + L_i X'_{ij} = A'_{ij} \Leftrightarrow X'_{ij} = \frac{A'_{ij}}{L_i + L_j}. \tag{D11}$$

Backtransforming to $\mathbf{X} = \mathbf{P}\mathbf{X}'\mathbf{P}^\dagger = \partial_\varphi \mathbf{K}^{-1/2}$ yields the desired derivative of $\mathbf{K}$ and subsequently of $\mathbf{M}$. To perform the described computation we need to know $\partial_\varphi \mathbf{K}^{-1}$ in Eq. (D8); however this quantity may be straightforwardly calculated when starting from the identity $\mathbf{K}\mathbf{K}^{-1/2}\mathbf{K}^{-1/2} = 1$, resulting in $\partial_\varphi \mathbf{K}^{-1} = -\mathbf{K}^{-1}(\partial_\varphi \mathbf{K})\mathbf{K}^{-1}$.

2. Mixing

In order to solve the saddle-point equations, a method to deal with a system of nonlinear equations $\mathbf{F}$ as a function of the variables (slave bosons and Lagrange multipliers) $\mathbf{x}$ has to be utilized as follows:

$$\mathbf{F}(\mathbf{x}) = 0. \tag{D12}$$

In the present work we tested several quasi-Newton techniques (e.g., Broyden,[53] modified Broyden,[54] etc.) to handle this numerically. Thereby from a starting guess for $\mathbf{x}$ the variables are updated via

$$\mathbf{x}_{(m+1)} = \mathbf{x}_{(m)} + \mathbf{J}^{-1}_{(m)} \mathbf{F}_{(m)}, \tag{D13}$$

since we want $\mathbf{F}_{(m+1)}$ to be zero to linear order. The Jacobian $\mathbf{J}$ is here defined as follows

$$J_{ij} \equiv -\frac{\partial F_i}{\partial x_j}, \tag{D14}$$

and is not calculated exactly (this would involve second derivatives and would lead to the Newton-Raphson method) but is computed at each step m via formulas which dictate several constraints on how $\mathbf{J}$ should evolve. In our numerical implementation we found the modified Broyden scheme to be well suited for the so far investigated applications Note that there is usually no need for explicitly fixing the gauge for the numerical solution of the saddle-point equations. The initial amplitudes of the variational parameters, i.e., slave bosons and Lagrange multipliers, at the start of the iteration, together with the choice of the atomic basis $|A\rangle$, always ensured proper convergence to one of the family of solutions within our implementation.

*frank.lechermann@physnet.uni-hamburg.de

[1] G. Kotliar, in *Strongly Interacting Fermions and High-T_c superconductivity*, edited by B. Doucot and J. Zinn-Justin (Elsevier, New York, 1995), Les Houches, Session LVI, p. 197.

[2] M. Imada, A. Fujimori, and Y. Tokura, Rev. Mod. Phys. **70**, 1039 (1998).

[3] A. Damascelli, Z. Hussain, and Z.-X. Shen, Rev. Mod. Phys. **75**, 473 (2003).

[4] M. R. Norman *et al.*, Nature (London) **392**, 157 (1998).

[5] M. Le Tacon, A. Sacuto, A. Georges, G. Kotliar, Y. Gallais, D. Colson, and A. Forget, Nat. Phys. **2**, 537 (2006).

[6] T. Maier, M. Jarrell, T. Pruschke, and M. H. Hettler, Rev. Mod. Phys. **77**, 1027 (2005).

[7] G. Kotliar, S. Y. Savrasov, K. Haule, V. S. Oudovenko, O. Parcollet, and C. A. Marianetti, Rev. Mod. Phys. **78**, 865 (2006).

[8] A. M. S. Tremblay, B. Kyung, and D. Senechal, J. Low Temp. Phys. **32**, 424 (2006).

[9] A. Georges, G. Kotliar, W. Krauth, and M. J. Rozenberg, Rev. Mod. Phys. **68**, 13 (1996).

[10] D. Sénéchal and A.-M. S. Tremblay, Phys. Rev. Lett. **92**, 126401 (2004).

[11] M. Civelli, M. Capone, S. S. Kancharla, O. Parcollet, and G. Kotliar, Phys. Rev. Lett. **95**, 106402 (2005).

[12] O. Parcollet, G. Biroli, and G. Kotliar, Phys. Rev. Lett. **92**, 226402 (2004).

[13] T. Li, P. Wölfle, and P. J. Hirschfeld, Phys. Rev. B **40**, 6817 (1989).

[14] R. Frésard and P. Wölfle, Int. J. Mod. Phys. B **6**, 685 (1992).

[15] C. Attaccalite and M. Fabrizio, Phys. Rev. B **68**, 155117 (2003).

[16] M. Ferrero, Ph.D. thesis, SISSA-Trieste, 2006.

[17] G. Kotliar and A. E. Ruckenstein, Phys. Rev. Lett. **57**, 1362 (1986).

[18] R. Frésard and G. Kotliar, Phys. Rev. B **56**, 12909 (1997).

[19] J. Bünemann, W. Weber, and F. Gebhard, Phys. Rev. B **57**, 6896 (1998).

[20] B. R. Trees, A. J. Fedro, and M. R. Norman, Phys. Rev. B **51**, 6167 (1995).

[21] X. Dai, G. Kotliar, and Z. Fang, arXiv:cond-mat/0611075 (unpublished).

[22] B. R. Bulka and S. Robaszkiewicz, Phys. Rev. B **54**, 13138 (1996).

[23] J. H. Shim, K. Haule, and G. Kotliar, Nature (London) **446**, 513 (2007).

[24] Y. Ono, M. Potthoff, and R. Bulla, Phys. Rev. B **67**, 035119 (2003).

[25] M. J. Rozenberg, Phys. Rev. B **55**, R4855 (1997).

[26] T. Pruschke and R. Bulla, Eur. Phys. J. B **44**, 217 (2005).

[27] K. Inaba and A. Koga, Phys. Rev. B **73**, 155106 (2006).

[28] J. E. Han, M. Jarrell, and D. L. Cox, Phys. Rev. B **58**, R4199 (1998).
[29] Y. Song and L.-J. Zou, Phys. Rev. B **72**, 085114 (2005).
[30] A. Koga, N. Kawakami, T. M. Rice, and M. Sigrist, Phys. Rev. Lett. **92**, 216402 (2004).
[31] A. Rüegg, M. Indergaard, S. Pilgram, and M. Sigrist, Eur. Phys. J. B **48**, 55 (2005).
[32] L. de' Medici, A. Georges, and S. Biermann, Phys. Rev. B **72**, 205124 (2005).
[33] V. I. Anisimov, I. Nekrasov, D. Kondakov, T. M. Rice, and M. Sigrist, Eur. Phys. J. B **25**, 191 (2002).
[34] A. Liebsch, Phys. Rev. B **70**, 165103 (2004).
[35] M. Ferrero, F. Becca, M. Fabrizio, and M. Capone, Phys. Rev. B **72**, 205126 (2005).
[36] H. Monien, N. Elstner, and A. J. Millis, arXiv:cond-mat/9707051 (unpublished).
[37] G. Moeller, V. Dobrosavljević, and A. E. Ruckenstein, Phys. Rev. B **59**, 6846 (1999).
[38] A. Fuhrmann, D. Heilmann, and H. Monien, Phys. Rev. B **73**, 245118 (2006).
[39] S. S. Kancharla and S. Okamoto, Phys. Rev. B **75**, 193103 (2007).
[40] M. Capone (private communication).
[41] M. Ferrero, P. S. Cornaglia *et al.* (unpublished).
[42] G. Biroli, O. Parcollet, and G. Kotliar, Phys. Rev. B **69**, 205108 (2004).
[43] G. Kotliar, S. Y. Savrasov, G. Pálsson, and G. Biroli, Phys. Rev. Lett. **87**, 186401 (2001).
[44] J. E. Hirsch, Phys. Rev. B **31**, 4403 (1985).
[45] N. Furukawa and M. Imada, J. Phys. Soc. Jpn. **61**, 3331 (1992).
[46] G. Fano, F. Ortolani, and A. Parola, Phys. Rev. B **42**, 6877 (1990).
[47] E. Dagotto, A. Moreo, F. Ortolani, D. Poilblanc, and J. Riera, Phys. Rev. B **45**, 10741 (1992).
[48] T. Kashima and M. Imada, J. Phys. Soc. Jpn. **70**, 2287 (2001).
[49] D. Rohe and W. Metzner, Phys. Rev. B **71**, 115116 (2005).
[50] T. Maier, M. Jarrell, T. Pruschke, and M. H. Hettler, Rev. Mod. Phys. **77**, 1027 (2005).
[51] X.-G. Wen and P. A. Lee, Phys. Rev. Lett. **76**, 503 (1996).
[52] M. Fabrizio (unpublished).
[53] C. G. Broyden, Math. Comput. **19**, 577 (1965).
[54] D. Vanderbilt and S. G. Louie, Phys. Rev. B **30**, 6118 (1984).
[55] In this paper, the chemical potential is usually included in the one-body part $\varepsilon^0_{\alpha\beta}$ of the local Hamiltonian.
[56] Note, however, that both sides of Eq. (24) have identical matrix elements between physical states.